ACTIVE HYDROGEN SENSING USING A PALLADIUM COATED OPTICAL FIBER BRAGG GRATING SENSOR

by

Matrika Bhattarai

B.A in Physics, Ithaca College, 2004

Submitted to the Graduate Faculty of

The School of Engineering in partial fulfillment

of the requirements for the degree of

Master of Science in Electrical Engineering

University of Pittsburgh

2006

UNIVERSITY OF PITTSBURGH

SCHOOL OF ENGINEERING

This thesis was presented

by

Matrika Bhattarai

It was defended on

September 25, 2006

and approved by

Kevin Chen, PhD, Professor, Electrical and Computer Engineering Department

Joel Falk, PhD, Professor, Electrical and Computer Engineering Department

Minhee Yun, PhD, Professor, Electrical and Computer Engineering Department

Thesis Advisor: Kevin Chen, PhD, Professor, Electrical and Computer Engineering Department

ACTIVE HYDROGEN SENSING USING A PALLADIUM COATED OPTICAL FIBER BRAGG GRATING SENSOR

Matrika Bhattarai, M.S.

University of Pittsburgh, 2006

The use of liquid hydrogen as a fuel in both ground and in space requires low-cost multi-point sensing of hydrogen gas for leak detection well below the 4% explosion limit of hydrogen. In this thesis, we demonstrate an agile multi-functional active fiber optical hydrogen sensor for all temperature operations. Fiber-optical hydrogen sensors offer a number of advantages over other hydrogen sensor including explosive proof, low-cost, multiplexing, and capability of working in hostile environments. They are very suitable for mission-critical applications such as for hydrogen sensing and leak detection in aerospace vehicles.

In this thesis, we demonstrate a multi-point, one-feed through, in-fiber hydrogen sensor capable of hydrogen detection below 0.5% concentration with a response time of less than 10 seconds. Our solution entails use of a fiber Bragg grating (FBG) coated with a layer of hydrogen-absorbing palladium which, in turn, induces strain in the FBG in the presence of hydrogen. The hydrogen-induced stress was detected by the shift of FBG wavelength. The responsivity of fiber optic hydrogen sensor was calibrated for hydrogen concentration from 0.1% to 10% and temperature range from -120^{o}C to 120^{o}C. The optimal sensitivity and response time of the sensor was found to be highly sensitivity to the temperature. The response due to the presence of hydrogen is imperceptible until the temperature reaches about -20^{o}C.

To develop a fiber-based hydrogen sensor for operation at all temperature, infrared power laser light carried by the same fiber containing FBG was used to induce localized heating in the

palladium coating which dramatically decreases sensor response time and increases the sensor's sensitivity at low temperatures. At -50^{o}C localized heating yields 57% of sensitivity of that at room temperature. This technology promises an inexpensive fiber solution for a multi-point hydrogen detection array with only one fiber feed-through operation for all-temperature hydrogen sensing.

TABLE OF CONTENTS

LIST OF TABLES

LIST OF FIGURES

ACKNOWLEDGEMENTS

I am very thankful to numerous people who made my research and course of study at the University of Pittsburgh a reality. Firstly, I am deeply indebted to my advisor Dr. Kevin Chen who has guided and supported me through the entirety of this work. Dr. Chen has poured in me an ocean of knowledge in the field of optical electronics. Without his astute guidance, none of this work would have been possible. Secondly, I would like to thank my fellow graduate research assistant, Michael Buric, for sharing his knowledge and for his immense guidance throughout the project.

I would like to express my gratitude to Dr. Joel Falk for introducing me to optical electronics and for the evaluation of this thesis. I would also like to thank Dr. Minhee Yun for taking his precious time to evaluate this work and for his invaluable discussions.

I am thankful to my fellow graduate research assistants, Chuck Jewart, and Zsolt Poole for their continuous support to my efforts. Special thanks go to Dr. Phil Swinehart and Dr. Mokhtar Maklad at Lake Shore Cryotronics for their support and plentiful interactions throughout the project. I would also like to thank Sandy Weisberg and Angela Ellis for their unending guidance throughout my academic career. Finally, I wish to acknowledge the support of my parents, my brother and sister for their encouragement and for being there.

1.0 INTRODUCTION

1.1 MOTIVATION

Fiber Bragg gratings (FBGs) have been significant components for many applications in fiber-optic communication and sensor systems. FBGs were first developed in the 1970's. In simple terms, a FBG is an optical fiber with a core index of refraction that has been modulated periodically or non-periodically over some portion of its length. It has an inherent property of being reflective at some particular wavelength of light due to the constructive and destructive interference formed as light passes through the changing index in the fiber. The central wavelength reflected by the FBG shifts with induced stretch and/or strain in the fiber, and this shift can be detected using an optical spectrum analyzer.

The fabrication of FBGs is simple and they are readily available commercially. By coating a FBG with a palladium layer, a hydrogen sensor can be built. When the palladium layer comes in contact with hydrogen, it forms a hydride (PdH_x), which causes swelling, stress and strain on the grating. This induces a change in the refractive index of the palladium coating, which in turn shifts the central reflected wavelength.

Hydrogen has been used as fuel in space vehicles and for numerous commercial applications. In such cases, hydrogen will be subjected to severe and unknown stresses over long lifetimes, and its storage and transfer on the ground exposes personnel and facilities to potential fire and explosion hazards, making hydrogen-leak detection necessary. Palladium is a well-

known sensing material specific to hydrogen. But at low temperatures, such as found near a cryogenic system or at high altitudes, sensitivity and response times are found to be severely degraded. Optical heating of the FBG will be implemented to improve performance (response time) at such low temperatures. Fiber optic sensors are explosion-proof and light-weight. They can be multiplexed, so a single fiber can replace many wires (single feed-through points).

The work described herein was motivated by the understanding that existent technologies could be applied to the hydrogen sensing problem in order to realize an inexpensive and accurate system. We intend to show that such a hydrogen sensor can be used for all-temperature operation.

Compared to electronic sensors, these active fiber sensors provide a number of appealing advantages:

- **One-fiber Solution:** Firstly, fiber optics inherently provides a network infrastructure. A sensor network with hundreds of nodes can be connected using a single fiber.
- **Easy to package**: The sensor elements are in fiber; and the transducers are on-fiber coatings. Additional cabling or metal contacts are not needed. It is a true one-fiber (one-cable) solution. This is in sharp contrast to electronic sensors requiring a large number of wires. In contrast; the benefits of tiny MEMS or other microelectronic sensors may be outweighed by the number of electrical feed-throughs, increased system complexity, and operational cost.
- **Suitable for harsh environments**: The proposed sensor network is immune to electromagnetic fields. It is low cost, has a long lifetime, and is capable of functioning in harsh environments such as high-*g* rocket launches, earth orbiting (extreme temperature cycling), and interplanetary exploration.

1.2 THESIS ORGANIZATION

Chapter 2 introduces the background information relevant to this thesis work. A brief theory and characteristics of FBGs, and a summary of grating fabrication techniques are included. Here, we will also discuss FBG strain sensors, the hydrogen-palladium system and various types of hydrogen sensors built in the past.

Chapter 3 talks about the experimental procedures used for the research that led to the thesis work. It begins with a detailed description of the fabrication of the FBG sensor used for hydrogen sensing, including the relevant output characteristics of the device. The chamber and the equipment used for the measurement of hydrogen at various concentrations are discussed as well.

Chapter 4 provides the experimental results obtained using the FBG hydrogen sensing setup. Various comparisons of results obtained using different experimental procedures are presented here.

Chapter 5 contains the conclusions made using the data presented in the experimental results section. It also includes a summary of the work presented in this thesis.

2.0 BACKGROUND INFORMATION

2.1 FBG THEORY AND CHARACTERISTICS

FBGs were first introduced in the 1980's after K.O. Hill discovered the technique to fabricate optical fiber gratings in 1978 [5]. Over the years, FBGs have had various applications in numerous optical telecommunication devices and sensor systems. We will briefly examine the physical principles governing the operation of a FBG, since it is the heart of the hydrogen sensing system presented in this thesis. Some of the techniques employed in the fabrication of FBGs will also be discussed.

A FBG is an optical fiber for which the index of refraction of the core is perturbed forming a periodic or non-periodic index modulation profile. A narrow band of the incident optical field within the fiber is reflected back, only at one particular wavelength called the Bragg wavelength (λ_B), by successive, coherent scattering from the index variations. Light at other wavelengths will pass through the fiber, and is transmitted with little attenuation. The Bragg or the reflecting wavelength is determined by both the period of the index change in the fiber (Λ), and the effective index of refraction (n_{eff}) of the core of the fiber. Hence, the Bragg condition is [1]:

$$\lambda_B = 2n_{eff}\Lambda \tag{1}$$

By modulating the periodic or non-periodic index change in amplitude and/or phase, different optical filter characteristics can be obtained.

The period (Λ) can be calculated for a grating by:

$$\Lambda = L / n \tag{2}$$

where L is the total length of the grating and n is the number of sequential index changes in that length for a linearly indexed common Bragg reflector. Now we can see clearly that if the length of the fiber is increased by mechanical stretching, the Bragg wavelength will shift towards longer wavelengths. What is less obvious as a result of stretching a FBG is that the index of refraction of the fiber also changes under strain. Figure 1 below shows the basics of operation of a FBG on an optical fiber.

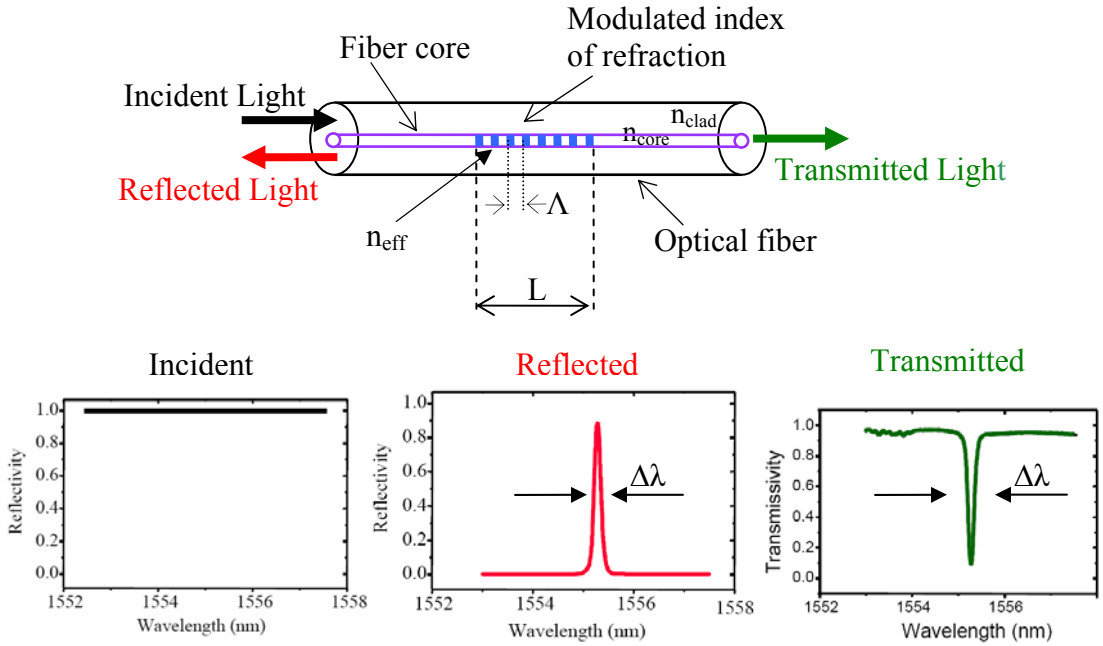

Figure 1: Operation of a FBG [2].

As seen in the figure, the reflection of the incident light occurs at a certain wavelength (λ_B). The reflection also has a finite width, known as the bandwidth ($\Delta\lambda$) of the grating. The bandwidth is usually between 0.01nm to 0.2nm based on the realized index change in a particular

grating as well as the overall grating length. The peak of the reflection spectrum shows the amount of light being reflected. This is called the reflectivity of the FBG, which is the ratio of the intensity of the reflected light over the intensity of the incident light, at the Bragg wavelength. For the transmission spectrum that is seen at the other end of the fiber, similar Bragg wavelength and bandwidth can be seen. This is known as the transmissivity of the FBG. The reflectivity of a FBG is the percentage of the ratio of intensity of the reflected light over the intensity of transmitted light, at the Bragg wavelength. Reflectivity can be changed by means of variation in the length of the FBG (changing number of grates or index changes) and the intensity of the index change in the grating.

The FBG can perform many primary functions, such as reflection and filtering, in a highly efficient manner. This versatility has stimulated a number of significant innovations [1, 15]. Engineers currently use FBGs to build sensors, multiplexers, de-multiplexers, filters, and other devices for various telecommunication applications, by applying the simple principles governing the variation in Bragg reflection spectra.

2.2 FABRICATION OF FBGS

In 1978 K.O. Hill *et. al*. [5] discovered that coherent standing waves from an Argon/Ion laser in a germanium doped silica optical fiber produce a periodic index change with the same period as the standing wave. Two things were discovered. Standard germanium doped silica telecommunications fiber can actually have its index of refraction altered via incident light of the correct wavelength. A Bragg reflector, which had been constructed before with multiple layers of different index material, could be produced inside an optical fiber utilizing this newfound

photosensitivity effect [16]. It was later determined that the photosensitivity effect is caused by rearrangement of the germanium bonding structure in the optical fiber on light exposure at the proper wavelength (157, 193, ~250 or 260 nm) [17]. Although a complicated setup was required to produce standing waves in optical fiber, and alterations to the characteristics of the inscribed grating were almost impossible, it was shown that inscription of optical fiber with a Bragg reflector was possible [5].

FBGs are fabricated by techniques that broadly fall into two categories: those that are holographic and those that are interferometric, based on simple exposure to UV radiation periodically along a piece of fiber. The later technique uses a beam splitter to divide a single input UV beam into two, interfering them at the fiber; the former depends on periodic exposure of a fiber to pulsed sources or through a spatially periodic amplitude mask. There are several laser sources that can be used for the grating, depending on the type of fiber used for the grating, the type of grating, or the intended application [5, 18]. The index of refraction in optical fiber could be altered via exposure to high energy pulses from a KrF laser normal to the length of the fiber [5]. These findings led to the phase mask inscription technique and also the point-by point inscription technique. These methods for grating production are discussed below.

2.2.1 Interferometric writing technique

One technique to be detailed for the inscription of FBGs is the interferometric technique. Meltz *et. al.* [19] had first shown that a holographic interferometer could be utilized to inscribe photosensitive fiber. In such a technique, a single UV beam from a KrF laser is split into two beams and subsequently brought together at a mutual angle (θ) by reflections from two UV mirrors as seen in figure 2 below. This produces a beam interference pattern of light and dark

fringes. Such an interference pattern may effectively inscribe a FBG. In addition, changing the wavelength of the laser source will change the distance between fringes, and thus the Bragg wavelength of the grating.

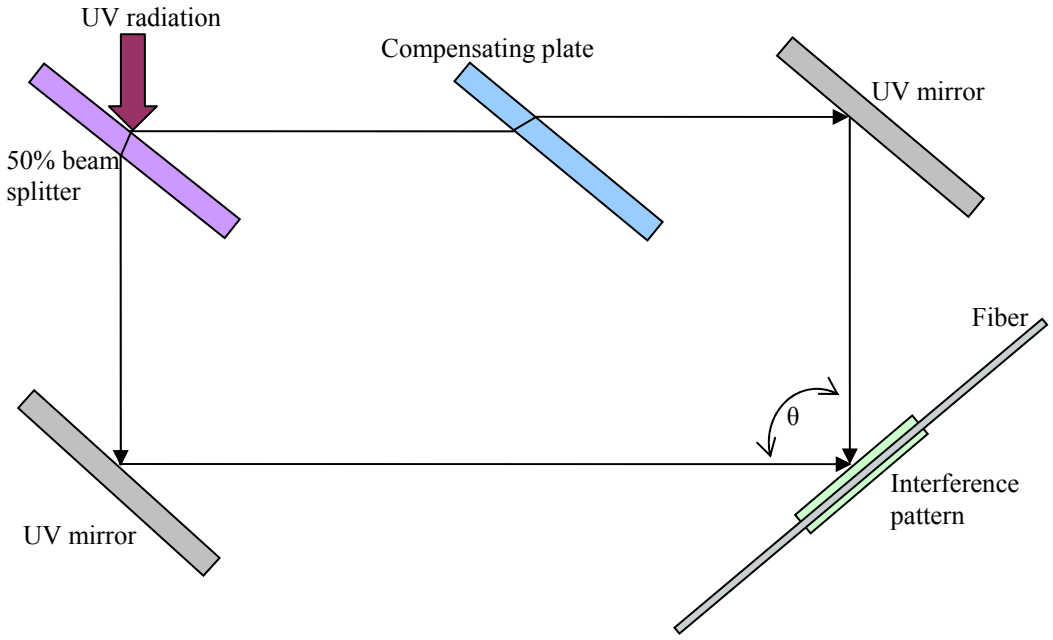

Figure 2: UV interferometer for writing Bragg gratings in optical fibers. An additional phase plate (mirror-blank) is seen on one arm to compensate for the path length difference. Reprinted from [18], with permission from Elsevier Press.

This method also allows the Bragg wavelength to be chosen independently of the UV wavelength as [18]:

$$\lambda_{Bragg} = \frac{n_{eff}\lambda_{uv}}{n_{uv}\sin(\theta/2)} \tag{3}$$

where λ_{Bragg} is the Bragg reflection wavelength, n_{eff} is the effective mode index in the fiber, n_{uv} is the refractive index of silica in the UV, λ_{uv} is the wavelength of the writing UV radiation, and θ is the mutual angle of the UV beams, as seen in figure 2 above. The interferometer is ideal for single-pulse writing of short gratings. Mechanical vibrations and the inherently long path lengths

in air can cause the quality of the interferogram to change over a period of time, limiting its application to short exposures. For low-coherence sources, the path difference between the two interfering beams must be equalized. A simple method is to introduce a blank mirror in one arm to compensate for the path imbalance imposed by the beam splitter [18], as seen in figure 2 above. Even though the interferometric writing technique is effective, it is much less used in practice than the phase mask or the point-by-point writing techniques. In principle, the diffraction grating used in reflection can replace the 50% beam splitter shown in figure 2. In this interferometer, two coherent beams are required, so that the reflection from a diffraction grating to divide the input UV beam into two is equally feasible [18]. However, a simpler method using a component called the transmission phase-grating, also known as the phase mask, is better for this application. It is discussed below.

2.2.2 Phase mask writing technique

The phase mask technique uses a high energy coherent KrF laser to illuminate a silica phase mask, which is usually constructed via ion beam etching and other micro-imprinting techniques. This provides a much easier inscription of fiber gratings. The phase mask is a relief grating etched in a silica plate. As shown in figure 3 below, the significant features of the phase mask are the grooves etched into a UV-transmitting silica mask place, with a carefully controlled mark-space ratio as well as etch depth. The principle of operation is based on the diffraction of the incident UV beam into several orders, m=…, -2, -1, 0, 1, 2… [18].

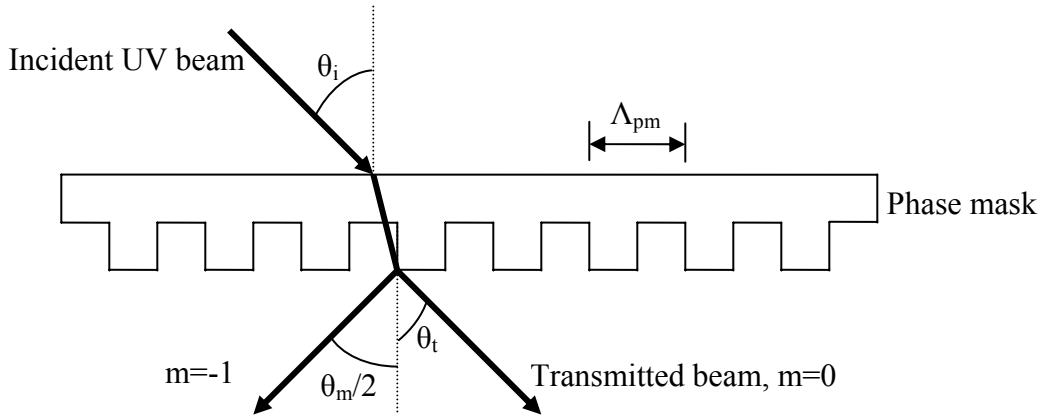

Figure 3: A schematic of the diffraction of an incident beam from a phase mask. Reprinted from [18], with permission from Elsevier Press.

The incident and diffracted orders satisfy the general diffraction equation, with the period Λ_{pm} of the phase-mask [18]:

$$\Lambda_{pm} = \frac{m\lambda_{uv}}{\left(\sin(\theta_m/2) - \sin(\theta_i)\right)} \tag{4}$$

where $\theta_m/2$ is the angle of the diffracted order, λ_{uv} the wavelength, and θ_i the angle of the incident UV beam. If the period of the grating lies between λ_{uv} and $\lambda_{uv}/2$, the incident wave is diffracted into only a single order (m= -1) with the rest of the power remaining in the transmitted wave (m=0).

When the UV radiation is at normal incidence ($\theta_i = 0$), as shown in figure 4, the diffracted radiation is split into m= -1, 0 and +1 orders. For two such beams of orders m= -1 and m=+1 brought together by parallel mirrors, the interference pattern at the fiber has a period Λ_g related by [18]:

$$\Lambda_g = \frac{\lambda_{uv}}{2\sin(\theta_m/2)} = \frac{\Lambda_{pm}}{2} \tag{5}$$

Then Bragg wavelength is found as [18]:

$$\Lambda_g = \frac{N\lambda_{Bragg}}{2n_{eff}} = \frac{\Lambda_{pm}}{2} \tag{6}$$

where $N \geq 1$ is an integer indicating the order of the grating period.

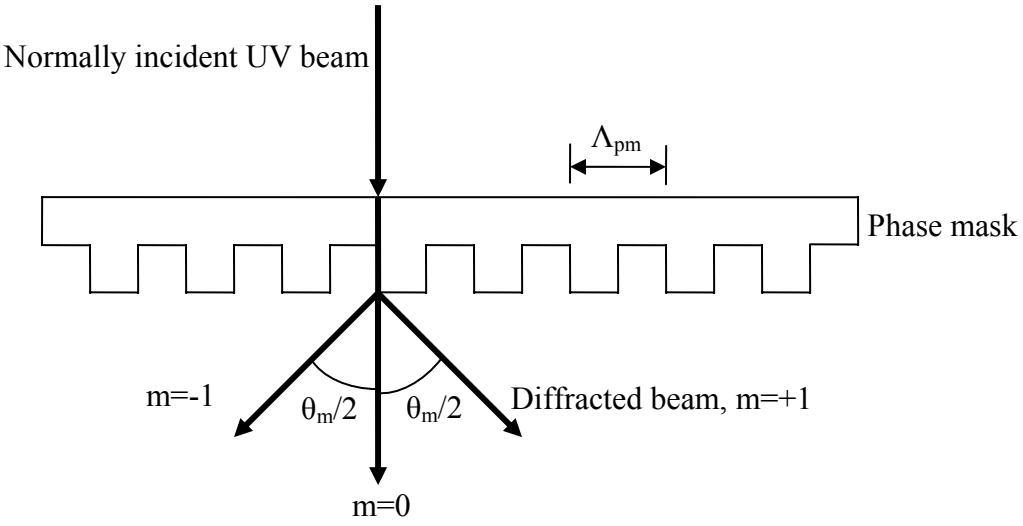

Figure 4: Normally incident UV beam diffracted into two ±1 orders. The remnant radiation exits the phase-mask in the zero order (m=0). Reprinted from [18], with permission from Elsevier Press.

Once inscribed with alternating opaque and translucent lines, the mask may be utilized to relegate the intensity of the KrF laser incident upon the photosensitive optical fiber [16, 18]. Using this method, a grating can be fabricated within seconds or minutes with little alignment after initial laser and mask setup [18].

2.2.3 Point-by-point writing technique

Point-by-point grating inscription offers a great deal of flexibility, while it does have a longer production time. This technique is similar to the phase mask technique described above. In this setup, a KrF laser is culminated in a tiny single slit. By illuminating a single spot at a time using this point-by-point writing technique, it is possible in principle to form a periodic refractive index grating. Practically, using positioning sensors linked to an interferometer, a grating with such periods can be written. This is only suitable for short gratings, due to the difficulty in controlling the translation stage movement accurately enough to make point-by-point writing of a first-order grating routinely practical [18].

The fiber is mounted on a mechanical stage that allows translation along the fiber length relative to the laser output slit. A single pulse from the laser is used to photosensitize one grate of the FBG before the fiber-stage is translated some length, by the use of mechanical rollers, for inscription of the next grate. In such a manner, FBGs with any arbitrary Bragg wavelength and grating length may be fabricated without the need for a number of different expensive phase masks. Unfortunately, the time required to write a grating in this fashion, including the continuous exposure and translation of the fiber, is much longer than that of a phase mask procedure requiring only a single exposure. However, this method is most suitable for long-period gratings, which do not require much demanding positional accuracy.

2.3 FBG STRAIN SENSORS

Most of the work on FBG sensors has focused on the use of such devices for providing quasi-distributed point sensing of strain or temperature [29]. FBGs are often used in either strain or temperature sensing, mostly in harsh environments. Longitudinal strain measurements in FBG sensors are based on the photo elastic effect, in which an applied mechanical strain influences the refractive index of the fiber material, i.e. silica. It is not feasible to attach bare FBG sensors, which are very fragile, to a structure in most applications. This requires the use of adhesive to attach the FBG element to a strong base.

The adhesive used has to be application specific. For example, in a high temperature environment, one would have to use an epoxy that would be best for this application. The first step in this process is to condition the surface, such as to sand it smooth, and to neutralize the surface so that it has proper pH, and then epoxy the FBG to the surface. Once the sensor is glued to the structure in the field it is very important to protect the fiber from damage. This can often be very challenging due to the distance that the structure may be from the measurement instrumentation. FBGs can be protected using cabling methods like Kevlar wrap and metallic sheathing [27].

The optical strain sensors provide an alternative to electrical strain sensors. These optical FBG sensors feature certain advantages like high accuracy, long-term stability, and better performance under harsh environmental conditions.

Hydrogen sensing using Pd coated FBG sensor works simply because of the formation of palladium-hydride (PdH_x), which creates swelling of the grating, and thus, the stress and strain in the grating. Thus, it is important for us to understand how the strain in the FBG can be sensed.

This section will discuss FBG tuning via mechanical stretching and heating. Earlier, we found the Bragg or the reflecting wavelength, which can be determined as:

$$\lambda_B = 2n_{eff}\Lambda \tag{7}$$

where Λ is the period of index modulation and n_{eff} is the effective index of the guided mode in the optical fiber. The period (Λ) can be calculated for a given grating by:

$$\Lambda = L / n \tag{8}$$

where L is the total length of the grating and n is the number of sequential index changes in that length for a linearly indexed Bragg reflector. The effective index of refraction, as well as the periodic spacing between the grating places will be affected by changes in strain and temperature. From the above two equations (7) and (8), it is pretty obvious that if the length of the fiber is increased via mechanical stretching, the Bragg wavelength will then shift towards longer wavelengths. Similarly, if the length is decreased due to mechanical stress, the Bragg wavelength will shift towards shorter wavelengths. However, one should also note that as a result of stretching a FBG, the index of refraction of the fiber also changes under strain. So, the strain response arises due to both the physical elongation of the sensor (and corresponding fractional change in grating pitch), and the change in fiber index of refraction due to photo-elastic effects. Similarly, temperature response arises due to the thermal expansion of the fiber material and the temperature dependence of the refractive index of the fiber [29].

The physics behind the stretching and straining of materials, including optical fiber, has been very well established [23]. If the Bragg wavelength of a FBG were to be shifted via mechanical stretching, we can refer to the physical properties of the optical fiber material itself in order to acquire information regarding the resulting changes in the material [24]. The shift in Bragg wavelength with strain and temperature can be expressed using [23, 29]:

$$\frac{\Delta\lambda_B}{\lambda_B} = \left(\left\{ 1 - \left(\frac{n^2}{2} \right) \left[P_{12} - \upsilon(P_{11} + P_{12}) \right] \right\} \varepsilon_z + \left[\alpha + \frac{\left(\frac{dn}{dT} \right)}{n} \right] \Delta T \right) \tag{9}$$

where ε_z is the applied strain, given in μm/m (μstrain), $P_{i,j}$ coefficients are the Pockel's (piezo) coefficients of the stress-optic tensor, υ is the corresponding Poisson's ratio, n is the core refractive index, α is the coefficient of thermal expansion of the fiber material (e.g. silica), and ΔT is the temperature change. Equation (9) above incorporates a factor, which is called the strain-optic constant (p_e) in the following discussion. This constant is given by:

$$p_e = \left(\frac{n^2}{2} \right) \left[P_{12} - \upsilon(P_{11} + P_{12}) \right] \tag{10}$$

The strain-optic constant, p_e, has an approximate numerical value of 0.22. In silica fibers, the thermal response is dominated by the *dn/dT* effect, which accounts for about 95% of the observed shift [29].

When a fiber is stretched, the Bragg wavelength will change solely due to the change in its index of refraction as [23]:

$$\Delta\lambda_B = \lambda_B (1 - p_e)\varepsilon_z \tag{11}$$

The applied strain (ε_z) is found by:

$$\varepsilon_z = \Delta L / L \tag{12}$$

where ΔL is the change in length of the grating and L is the original length of the grating. In equation (11) above, the strain-optic constant (p_e) is typically about 0.22 for silica fiber material. In general, the wavelength change due to the actual change in periodic length will be only about 6% of the change brought about by the change in the index of refraction in the fiber. In performing mechanical stretching of a FBG, care should be taken so as not to exceed the

deformation strain of the fiber. The deformation strain of the fiber is usually greater than 3500 μstrain (0.35% change in length) [16, 28]. In fact, the large yield strain of silica fibers makes them ideal for use in strain gauges commonly used in structural strain sensing [28].

Another effective method for wavelength tuning of a FBG is to alter the temperature of the grating. One should still note that most of the effect resulting from temperature changes in silica fiber is due to changes in the refractive index of the fiber, and not simply thermal expansion. Silica presents thermo-optic effect, in which the refractive index is sensitive to the temperature variation. A certain change in temperature, ΔT, results in change in the Bragg wavelength, given by [23]:

$$\frac{\Delta\lambda_B}{\lambda_B} = (\alpha + \xi)\Delta T \tag{13}$$

where α is the thermal expansion coefficient and ξ is the thermo-optic coefficient. In equation (13), α, which has an approximate value of 0.78×10^{-6} for silica, is given by [30]:

$$\alpha = \left(\frac{1}{\Lambda}\right)\left(\frac{d\Lambda}{dT}\right) \tag{14}$$

The thermo-optic coefficient, ξ, with an approximate value of 8.85×10^{-6} for Germania-doped silica core fiber, can be found as:

$$\xi = \left(\frac{1}{n}\right)\left(\frac{dn}{dT}\right) \tag{15}$$

Combining both the effects on Bragg wavelength shifts due to strain (equation 11) and temperature (equation 13), considering longitudinal strain (along the fiber axis) and an effective photo elastic constant p_e, we can come up with [23]:

$$\frac{\Delta\lambda_B}{\lambda_B} = (\alpha + \xi)\Delta T + (1 - p_e)\varepsilon_z \tag{16}$$

For a standard silica fiber, one would get [23, 30]:

$$\frac{\Delta\lambda_B}{\lambda_B} = 8.85\times10^{-6}\Delta T + 0.78\times10^{-6}\varepsilon_z \tag{17}$$

Hence, as determined by the above equation (17), a change in temperature by 1^{o}C would cause about a similar wavelength shift as a stretch of 10μm/m (μstrain or 0.001% change in length) longitudinal strain [16, 18, 23]. For a typical optical fiber, P_{11}=0.113, P_{12}=0.252, υ =0.16, and n=1.482 [30]. Using these parameters and equation (10) above, the expected sensitivity at ~1550nm is a 1.2pm shift in the Bragg wavelength as a result of applying 1 μstrain to the Bragg grating. From equation (17), it is very clear that the index change is by far the dominant effect.

Thermal compensation in strain measurements using FBG sensors is one of the key issues in the technology and several designs have been implemented to cope with it [23]. The significant limitation of FBG sensors is the dual sensitivity to strain and temperature. This creates a problem, since a sensor system designed to monitor strain will be affected by temperature variations along the fiber path. This can cause inconsistent readings. In order to get rid of this effect, reference gratings along the fiber array can be used. These gratings can be in thermal contact with the structure, but will not respond to any strain changes. Using this method, the difference in the wavelength shifts on the two FBGs at a certain point along the fiber path can provide the actual wavelength shift in the Bragg wavelength caused only by strain changes. Strain sensing is important in bridges, buildings, piers, and numerous other applications.

2.4 HYDROGEN PALLADIUM SYSTEM

Hydrogen has a very high potential for forming an explosive mixture with air or oxygen. It is stored in liquid (cryogenic), hydride or gaseous forms and has to be handled very carefully, which is commercially done using fuel systems tailored to the task and space vehicle. In the past, hydrogen sensing systems used resistance or silicon diode sensors, which involve multiple electrical wires feed-through into the hydrogen tank, or wires in the vicinity of the tank where the lower explosive limit (LEL) of about 4% H_2 in air might be reached. The FBG sensor system requires few feed-through penetrations. In addition, the sensors will be most cost-effective if many sensors can be multiplexed from the same instrumentation and if more than one parameter can be detected, such as liquid level, temperature and strain in addition to the direct detection of hydrogen gas. FBG sensors fit these requirements. The multiplexing capabilities of the FBG sensors is not altered by the addition of a palladium coating and the reliability of the in-fiber gratings will remain high because splices, adhesive joint and thinning or weakening of the fiber will not be necessary.

Since the LEL of hydrogen in air is about 4%, it is desirable that an alarm be sounded at as low a concentration and as fast as possible. The work in this thesis includes a multi-point in-fiber hydrogen sensor capable of detecting as little as 0.5% H_2 in N_2 with a response time of less than 10 seconds.

Palladium is one of the noble metals of the platinum group. It has the unique ability to absorb many times (up to 900 times) its own volume in hydrogen under the right conditions, and, further, the effects are very specific to hydrogen. The absorbed hydrogen causes the formation of palladium hydrides. The hydrogen and the hydrides cause reversible physical (swelling) and chemical changes that can be sensed electrically and optically.

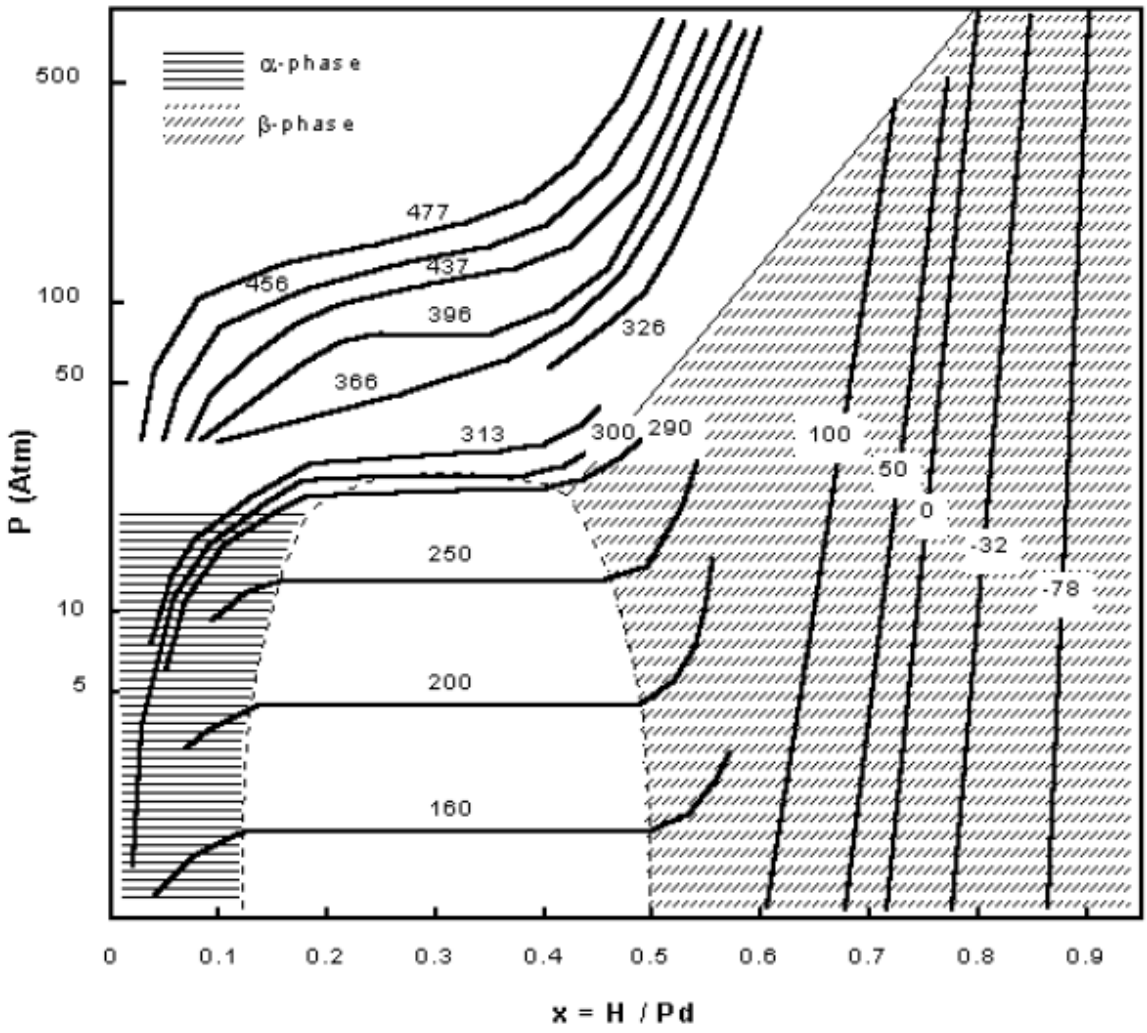

Figure 5: 'Pressure–composition' isotherms for palladium versus the absorption of molecular hydrogen for different temperatures in ^{o}C (from Lewis [3]). Reprinted from [11], with permission from Elsevier Press.

As seen in figure 5 above, for each isotherm corresponding to temperature lower than 300^{o}C, the palladium hydride formed can be either at an alpha (α) phase or a beta (β) phase, depending on the pressure, and the atomic ratio of hydrogen in palladium. These two different phases are separated by an isopressure zone.

For each isotherm, for pressures lower than the isopressure, the hydride is in α phase, while it is in β phase for pressures higher than the isopressure, as seen in the figure above. The isopressure zone is the phase transition from α to β for which both phases coexist without miscibility [11]. For temperatures over 300^{o}C, there is no isopressure zone and coexistence of the phases does not occur. Crystallographic modifications are caused by the hydration of palladium. These modifications are much different from the atomic distortions seen for solid solutions. The crystallographic modifications still keep the face centered cubic symmetry of the pure palladium, but with an increase of the lattice parameter up to 3.5% in the β phase [11]. The increased lattice parameter causes an increase in the thickness of the palladium layer and sometimes causes reversible surface cracks.

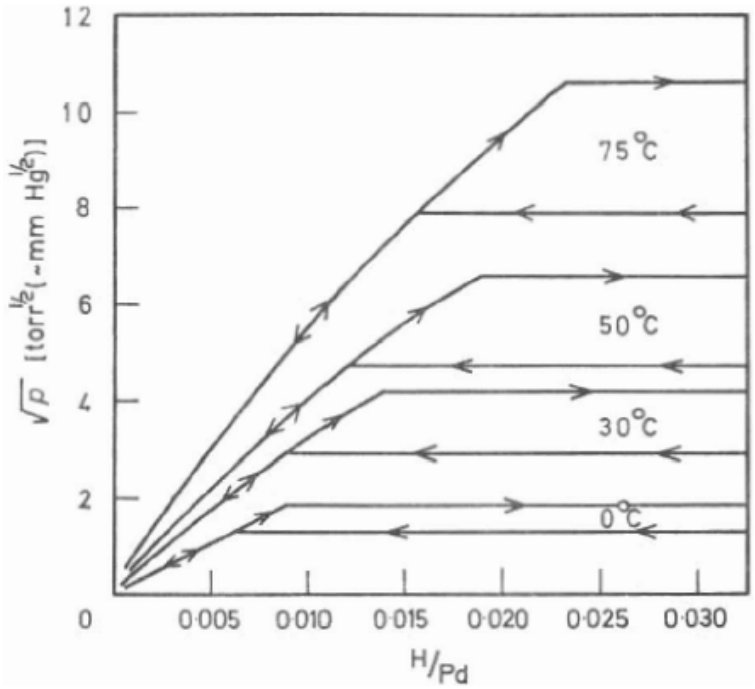

Figure 6: Hysteresis of pressure- Composition relationships over a lower range of temperatures – after Wicke and Nernst (1964). [3]

The temperature/pressure/composition data from the phase diagram above can be used for determining the operating regime necessary for viable sensors.

It is interesting to note that there are conditions under which irreproducible behavior will be encountered. These include structural and phase changes (α & β phases, as seen in figure 5 above, causing hysteresis) and surface contamination or "poisoning." Hydrogen must dissociate efficiently on the Pd surface in order to diffuse into the bulk.

For a good hydrogen sensor, it is desirable to be able to detect the hydrogen while the Pd/H composition is such that the hydride is in α phase. Initially the hydride at room temperature and atmospheric pressure is in α phase. As the H/Pd atomic ratio increases, with the increase in the hydrogen concentration, the hydride will eventually be in β phase.

2.5 EVOLUTION OF HYDROGEN SENSORS

Various electrical sensors based on the change of resistivity of Pd have been developed over the years [6-8], including recent excursions into the nano-scale arena [9]. Because of their explosion proof nature, the desirability of fiber optic sensing has been recognized in recent years and more effort has been placed in the development of optical sensors, especially types that can be interrogated remotely over fibers. Amongst the several methods used for gas detection, there are two different principles that use optical detection of hydrogen. One is based on the direct interaction between the hydrogen gas and the optical wave leading to spectroscopic analysis via infrared absorption or Raman scattering. The other principle uses the information from the optical wave given by the interaction between hydrogen and a transducer, which usually is a palladium layer. C. M. Davis *et. al*. [20] reported numerous devices where the absorption of hydrogen by a thin layer of palladium deposited on a waveguide led to the modification of its crystalline structure and consequently the change in the effective index of the guided wave.

Types that have been investigated include Pd mirrors and interferometers (using mirrors on the end of the fiber) [10, 11], surface plasmon resonance on multimode fibers [4], evanescent fields from tapered or thinned fibers that detect changes in real and imaginary parts of the refractive index of palladium hydride [12-13], and wavelength shifts due to strain induced in FBGs and Long Period Gratings (LPGs) by the swelling of Pd coatings [14]. Among the several methods that have been demonstrated, the most significant were based on surface Plasmon resonance [4], intensity variations by means of electro-chromatic materials [21] or interferometric measurements [20], and FBGs (using Pd micro-mirror deposited at the output end of a multimode fiber [11], and elasto-optic FBG sensor [14]). M. A. Butler [10] first demonstrated the interferometric optical fiber sensor for the detection of hydrogen in 1984. The

sensor was an interferometer with one arm coated with a palladium film. In the interferometer, the optical path length of the sensing arm changes when it is exposed to hydrogen or when its temperature is increased. This change in the optical path length shifts the fringes at the output of the interferometer and, hence, it can be detected. This sensor is quite complex and offers no multiplexing capability [14].

Since Butler and Ginley discovered the FBG sensor based on the change in the elastic property of Pd during H_2 absorption, there has been a fast-paced track in the development of devices accurate for remote sensing for local and volumetric detection of hydrogen with lower ignition risks and hazards near the sensing area [11].

M. A. Butler has also shown a new principle for hydrogen detection based on the variation of the reflectivity of a metallic micro-mirror deposited on the cleaved output end of a silica multimode fiber in 1991 [22]. This device provided both remote sensing and good performances, (sensitivity, wide range, magnitude of the response, and repetitivity) compared to the other sensors used for the optical detection of hydrogen. However, no information was provided on the response time and this sensor had only been operated at room temperature. Although the micro-mirror sensor is simple and inexpensive, its multiplexing capability is limited.

In 1999, Sutapun *et. al.* [14] have shown a Pd-coated elasto-optic FBG sensor for multiplexed hydrogen sensing. The long term dependency and temperature dependence of the sensor was still being investigated. They were able to show linear sensitivity for 0.3-1.8% hydrogen concentration. Their measurements were taken at room temperature, and the response times were not provided.

Bevenot *et. al.* [11], in 2000, built a sensor based on the variation of reflectivity of Pd micro-mirror deposited at the output end face of a multimode fiber. They monitored optical heating of the sensor using a high power laser diode to keep up the performances in the wide range of temperatures between -196^{o}C to 23^{o}C. For hydrogen concentration of 100%, they showed a response time of less than 5 seconds while for 4% H_2 concentration, it was around 40 seconds. They were able to show that at a very low temperature of -196^{o}C, with optical heating of the sensor using a high power laser diode, it was possible to sense 4% H_2 concentration (LEL) within 5 seconds. Einfeld [31] has shown an FET hydrogen sensor in 2002 and Hunter *et. al.* [32] have shown a hazardous gas detection technology for aerospace and commercial application using MEMS (Micr0-Electro Mechanical Systems) based technology.

In addition, Guemes, *et. al.* [25], have recently compared three of the optical methods. A paraphrased chart of their conclusions is given in Table 1.

Table 1: Comparison chart of optical hydrogen detectors [modified from 25].

	FBG, Thick Pd	Evanescent Taper, Thin Pd	Micromirror, Thin Pd	Surface Plasmon, Thin Pd
Measurement mechanism	Wavelength Shift (absolute)	Transmission (not absolute)	Reflection (not absolute)	Transmission (not absolute)
Response Time, 300K	90 sec. ($\Delta\lambda$~50pm)	16 sec.	erratic	74-150 sec.
Response Time, 240K	900 sec.	140 sec.	Not measured	Not measured
Reproducibility	Good	Low	Very low	Good
Repetitivity (Cycling?)	Yes	Yes	No	Yes
Multiplexibility	Yes	No	No	Limited
Robustness	Excellent	Poor	Easy to handle	Poor
Cost (time to manufacture)	Very High (40 hr)	High (8 hr)	Very low (3 min.)	Medium

There are a few comments that need to be made about the table above. The measurements were taken at room temperature and atmospheric pressure, and the response times were for 4% H_2 concentration in N_2. Pd thicknesses from 100nm to 500nm produce strain responses, especially in LPGs [11], which produce shifts of 2nm (very large signal) at 4%H_2 concentration. We will be using 150nm and 350nm Pd coated FBG for our hydrogen sensors. Absorption (transmission and reflection), or amplitude measurements have never been practical in the past. Fiber bending losses, dirty connectors and the like cannot be distinguished from the signal, which leads to inaccuracies. Even though Guemes et. al, say that the cost of FBG is very high; we have found this not to be true. The current cost of simple recoated FBGs is less than $50, and the additional processing for Pd coating should not more than double the cost. So, in fact, Pd coated FBG sensors seem to be the most viable technology for hydrogen sensing. The response times in the above table seem to be very high; this is so because none of those works summarized above used swept lasers, which can deliver about 50 times better accuracy and resolution. With the use of high power laser, we expect to see much lower response times. It is also important to note that since FBGs are fabricated in the fiber by outside exposure with a powerful excimer laser, they in general do not weaken the fiber and do not increase the fiber diameter much when recoated. The other factor, their absolute wavelength shift signal makes the FBGs optically reliable for accurate sensing purposes. The other sensors do not have absolute measurement mechanisms, which makes them less reliable than the FBG sensors.

2.6 ACTIVE HYDROGEN SENSOR POWERED BY IN-FIBER LIGHT

The fiber heating concept is shown in figure 7 below. The hydrogen-specific sensor unit is based on the Pd-coated FBG sensor illustrated in figure 7(a). A palladium film was first coated on a standard telecommunication fiber. As a well-known and excellent hydrogen-absorbing material, palladium films swell after hydride formation, which in turn produces strain in the FBG. The FBG response to the strain can be measured as a resonant Bragg peak wavelength shift. These FBG-based hydrogen sensors possess some important advantages for mission-critical monitoring tasks such as space shuttle hydrogen delivery systems. These advantages include low manufacturing cost, totally immune to electromagnetic fields (EMFs), long lifetimes, high sensitivity, and the capability of working in harsh environments. Miniaturized structures and low transmission losses in optical fibers enable the deployment of sensor arrays for multi-point and long-distance remote sensing.

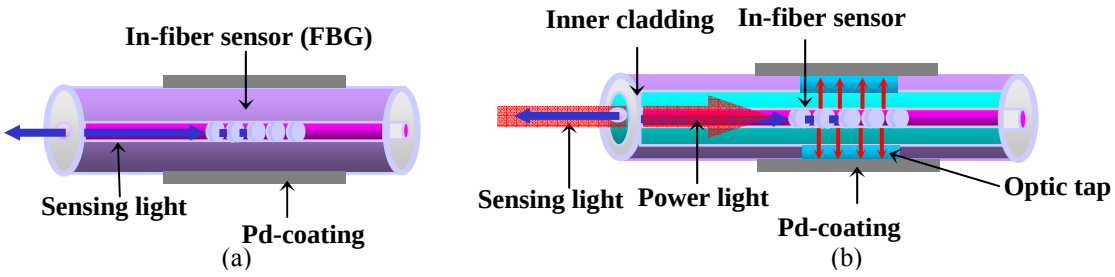

Figure 7: (a) Schematic of a traditional passive Pd-FBG sensor. (b) Active in-fiber grating sensor powered by light. The resonant wavelength, chirp, temperature, and birefringence can be adjusted by the high-power light.

Despite the advantages of purely optical fiber components, performance and application diversity have been limited by their total passivity. Passive sensor elements do not support active adjustment of sensing parameters to adapt to a changing environment. In this particular sensing application, the reaction rate for Pd-hydride formation has an exponential dependence on the temperature ($T<127^{o}C$). Most Pd-based sensors do not respond to hydrogen at the low temperatures required by most of the hydrogen fuel delivery systems. The inability to change a standard hydrogen sensor's temperature will completely diminish its performance in this temperature region.

In order to recover the Pd-FBG sensor's performance, we plan to locally heat the sensor to $150^{o}C$ operational temperature while in a cold environment for optimal sensor performance. Thus far, electricity has been the only form of energy used to power in-fiber devices. An electrical cable must run along with the optical fiber to supply this heat energy. Additional cabling, however, leads to many problems including an increase in manufacturing cost due to the additional on-fiber electrical contacts and feed-throughs, the need for delicate packaging, and the elimination of electromagnetic immunity. Such fiber components are no longer suitable for use in hostile environments and in fuel systems mostly used in the space mission.

In this thesis, we demonstrated the concept that active FBG sensors can be directly powered by in-fiber light as illustrated in figure 7(b). In contrast to a passive sensor (figure 7a); optical power is delivered together with a sensing signal through the same fiber that contains FBGs. Optical taps are fabricated in desired sections of the optical fiber to release high-power laser light as an energy source to heat a Pd-coating to the optimal operation temperature. The optical characteristics of the Pd-FBG sensor can then be adjusted using this optical energy. By eliminating the electric cabling, on-fiber electric contacts, and delicate packaging, dramatic

functional enhancement of FBG sensors can be achieved without compromising any of the intrinsic advantages of in-fiber passive sensors.

Along the course of this project, several benchmarks were set in order to quantify the success or failure of the sensing system. Among these benchmarks were: a 1% or better lower detection limit, low temperature detection capabilities, and leak location capabilities. As we intend to show in the results that follow, sensors were successfully fabricated in various optical fibers with detection limits as low as 0.5% or better. It will also be shown that multiplexing of multiple sensors in the same fiber could be possible, enabling leak location with multiple sensors and only one fiber send line or feed-through point. Finally, this novel approach to sensor heating using in-fiber laser light will allow sensor operation at low temperatures with extremely fast response times.

In the following sections, detailed experimental procedures, results on sensor fabrication, calibration, optical heating, and the demonstration of hydrogen sensing will be elaborated upon.

3.0 EXPERIMENTAL PROCEDURES

In this section, we will discuss the fabrication of the FBG sensor and then the method used for coating the Pd layer onto the grating. A brief explanation about the chamber used for the detection of hydrogen is also provided. We will also introduce optical heating using a laser source for fast detection of hydrogen and also for fast degassing using optical heating.

3.1 SENSOR FABRICATION

In the course of the research, a number of viable hydrogen sensors in optical fiber were produced with the help of Lake Shore Cryotronics, Inc. The following is a brief review of the procedures used for fabrication of such sensors. It can be shown that technologies implemented in the construction of sensors described herein are both scaleable and easily reproducible with some capitol equipment investment.

The fiber used in this work is specialty double-clad fiber, as shown in figure 8 below. To enable the deployment of active fiber sensor arrays for long-distance sensing and other practical applications, we have collaborated with a specialty fiber manufacturer (Stocker Yale Inc., Salem, NH) for the fabrication of a double-clad fiber.

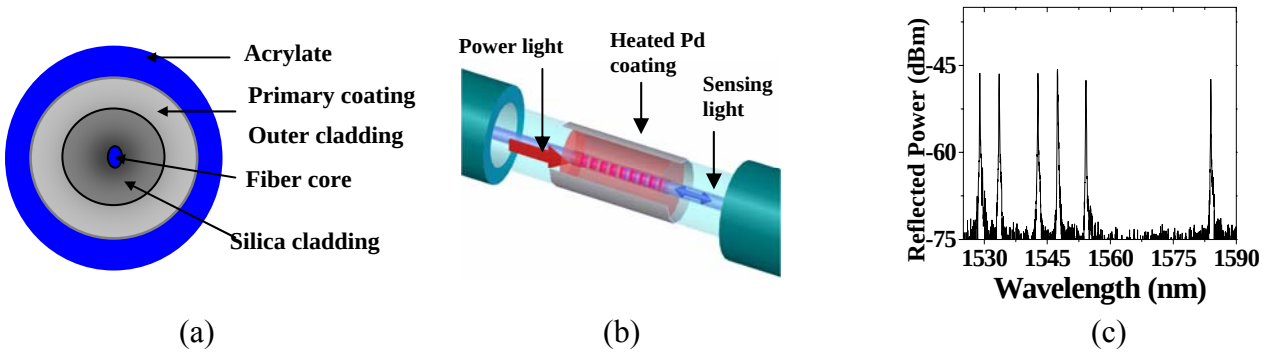

Figure 8: (a) Sketch of the double-cladding fiber provided by Stocker Yale Inc., (b) Schematic of active FBG hydrogen sensor, (c) Reflection spectrum of 6-FBG array inscribed in the double-clad fibers.

This fiber has an 8-μm diameter photosensitive Ge/P co-doped silica core shown in figure 8 (a). The fiber was dual-coated with UV curable acrylate with a diameter of 245 μm. The primary coating has the refractive index lower than that of pure silica, and serves as the second cladding with 0.48 N.A. The inner cladding of the fiber can be used to deliver high-power laser light to any point along the fiber for on-fiber optical heating.

The first step in the fabrication of this special breed of H_2 sensors is to write a FBG into a length of optical fiber. The primary method used here, at the University of Pittsburgh, for inscription of the grating is a well proven phase-mask technique. In such a technique, double-clad fibers were loaded with hydrogen at high pressure (1500 psi) for a period of 5 days to photosensitize the fibers. After photosensitization, the fiber is then placed behind a silica phase-mask for illumination by the excimer source. Annealing is then accomplished at 150^{o}C for 24 hours to permanently stabilize the inscribed grating. Figure 8 (c) shows the reflection spectrum of a FBG array containing 6 FBGs. More FBGs can be easily inscribed in the same fiber using phase masks with various periods. Figure 9 shows the grating writing setup at the University of Pittsburgh.

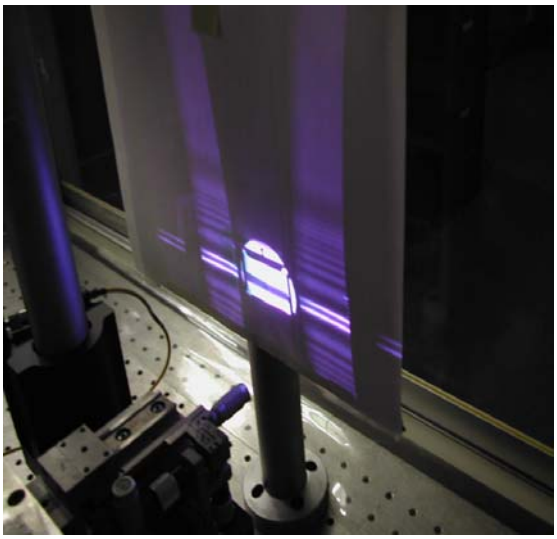

Figure 9: The diffraction pattern of the fiber during the FBG writing.

After a Bragg grating has successfully been written in a fiber, it is next necessary to apply a coating of Palladium to the surface of the FBG in order to induce strain in the fiber in the presence of hydrogen. This coating is a precise process which has been perfected by Lakeshore Cryotronics Inc. Therein, the fiber is first cleaned to remove surface contaminants. Next, the fiber is loaded into a jig allowing transverse mounting in a magnetron sputtering machine. Figure 10 below shows the fixture utilized for sputtering. In the sputtering machine, Ultra High Vacuum (UHV) is drawn, allowing the flattest most defect free coating possible. In order to allow adhesion of the Pd sensing layer, a thin (20nm) layer of Tantalum is first deposited on the fiber. On top of the Tantalum layer, a thick layer (150nm-350nm) of Palladium is deposited. A number of different coating configurations and thicknesses were deposited on FBGs for testing and evaluation.

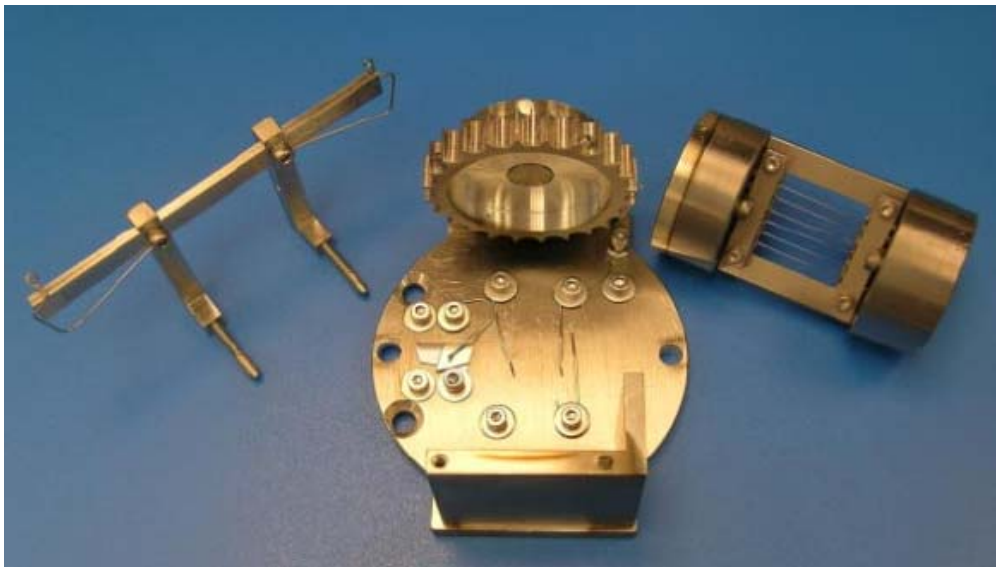

Figure 10: Components for fiber sputter coating: hanger on the left; carrier plate on the center and rotation wheel on the right.

Wire clips on carrier plate hold flat substrates used as witness samples to measure metal thickness. Figure 11 shows the film holder drum and the drum installed on the carrier plate. The fiber is coated only in the frame area (2.5cm), where the FBGs are located, as shown in figure 11. The excess fiber is coiled up in the drums at the ends. The fiber is then spliced to lengthen it, and a connector is added for testing.

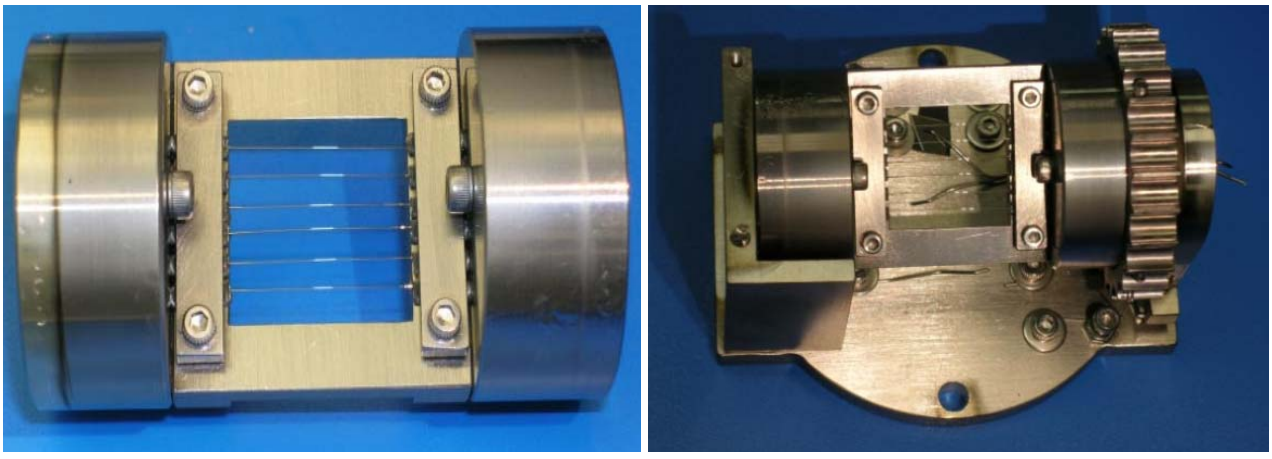

Figure 11: Sputter Coating Fixture provided by Lake Shore Cryotronics Inc.

Figure 12 below shows the pictures of the sensor taken at the junction of the Pd coated FBG and the silica fiber. Figure 12 (a) was taken at a magnification of 200 times while figure 12 (b) was taken at 400 times magnification.

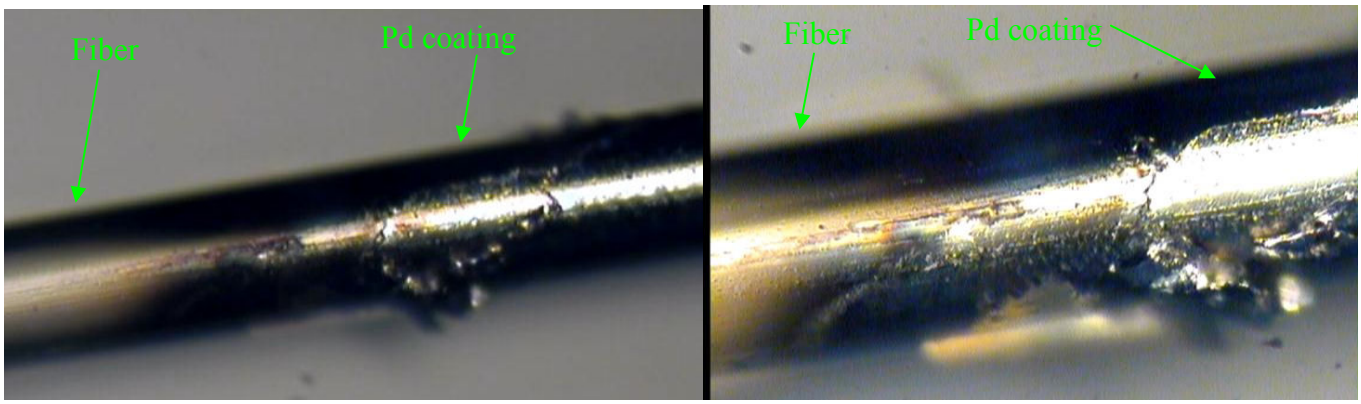

Figure 12: Microscope pictures of Pd coated fiber: (a) magnified 200 times, (b) magnified 400 times.

3.2 TEST EQUIPMENT AND EXPERIMENTAL SETUP

After the fabrication of a vast number of optical hydrogen sensors for evaluation, it was necessary to construct an environmental chamber and experimental platform on which to test each sensor. The basic concept therein was to reproduce environmental characteristics of interest, as well as provide variable hydrogen content for sensor characterization. To facilitate precise environmental control, a chamber was constructed to house as many as four sensors in a temperature and pressure controlled environment. This chamber is shown in figures 13 and 14. Figure 14 shows the steel core of the chamber (in red) before the steel casing (as seen in the pictures on figure 13) was integrated on top of it.

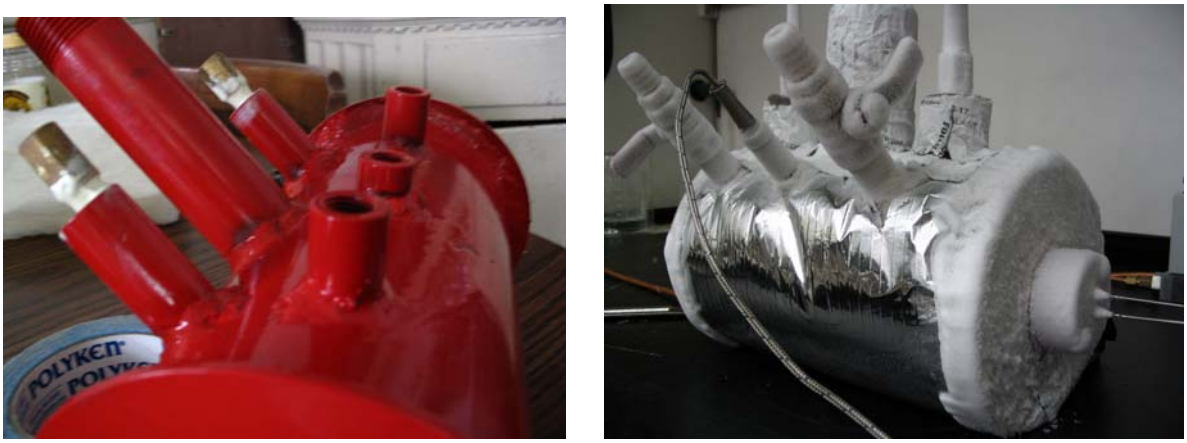

Figure 13: H_2 Sensor Test Chamber

Figure 14: Close up view of the H_2 sensing chamber core before installing the outer steel casing.

The gas input and output ports, thermocouple probe, convection pressure gauge, and mass flow controllers (on the right) can be seen in figure 14. Several important features should be noted in the figure. Firstly, four small pieces of 130µm inner diameter 10cm long stainless steel capillary tubing provide entry ports for fiber without allowing excessive air leakage from the outside. In practice, vacuum grease was used to seal the test fiber to the capillary tubing,

providing an air tight seal that will withstand positive or negative pressures due to the small sealing diameter. These pieces of capillary tubing are press-fit into the chamber's steel end-caps. These caps are secured on the ends of the chamber with butyl o-rings and four 10-32 machine screws. These end caps seal a central 3cm inner diameter chamber in which the sensor resides during testing. This central chamber is surrounded by a 15cm outer diameter steel cylinder for temperature regulation. This outer cylinder is equipped with ports that allow addition of either liquid nitrogen for cryogenic cooling, or circulated ethylene glycol for regulated heating. The temperature is measured via a thermocouple, while the internal chamber pressure is measured with a Pirani vacuum gauge.

The remainder of the test setup consisted of equipment necessary to support the central test chamber. Primarily, this included gas delivery and regulation equipment, as well as optical sources and measurement devices. The test chamber was fed via a tank of pure nitrogen, and a tank of 10% hydrogen / 90% nitrogen. These two tanks were pressure-regulated down to 50 psi, and used to drive two mass/flow controllers. These controllers provided between 0 and 125 cc/min of either gas at the same time, allowing variable hydrogen/nitrogen gas mixes from 0-10% at the same flow rate. A digital mass/flow controller driver and power supply was used to operate both controllers. Some of the support equipment, as shown in figure 15, are the broadband source on top, the optical spectrum analyzer (OSA), laser diode on top of a cooling fan, D.C power supply, temperature gauze and digital mass/flow controller driver.

Figure 15: Test Chamber Support Equipment

Several key pieces of optical equipment were necessary to operate and characterize the H_2 sensor. A schematic diagram of this equipment is shown in figure 16 below. Light from a high-power laser diode (LD) was coupled into a multimode fiber, which is fusion spliced to the double clad fiber. To interrogate the sensor, it was connected to a broadband light source and an Optical Spectrum Analyzer (OSA in the figure below) (Ando 6317C) via a circulator. This allowed precise measurement of the FBG's reflected spectrum. A small infrared (910nm) high power (1.5W) fiber laser was connected to the other end of the fiber to provide the ability to heat the sensor remotely.

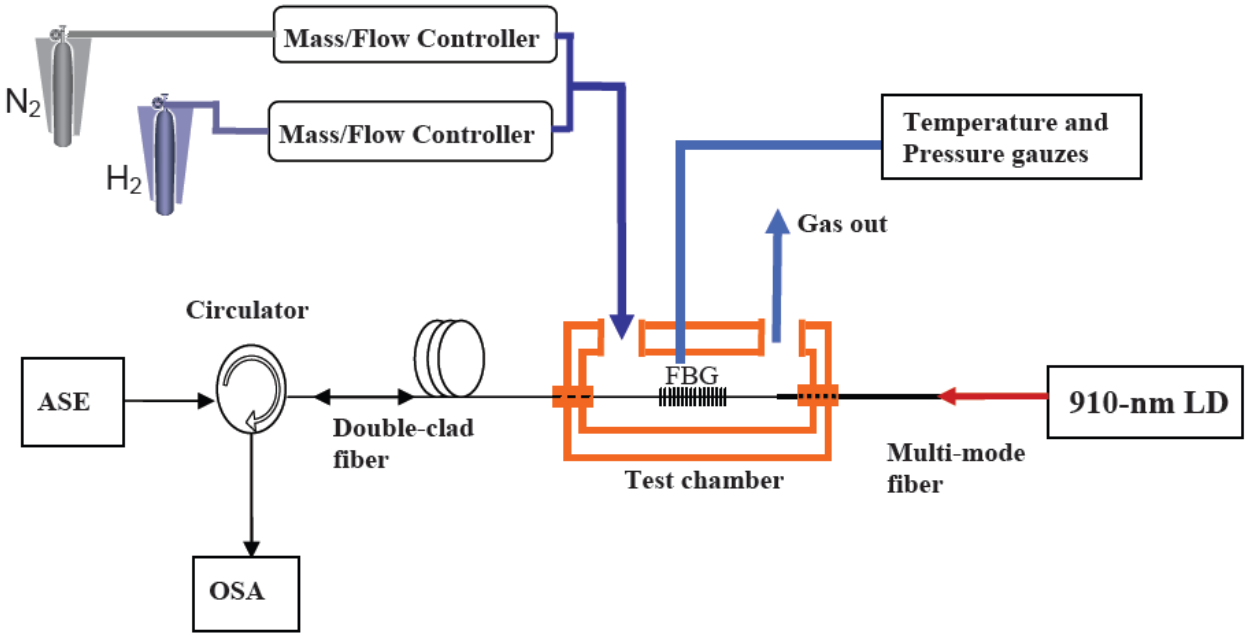

Figure 16: Prototype of a heated FBG sensor in a double clad fiber powered by light.

Local sensor heating was accomplished via an infrared laser coupled to the sensor. Initially, the laser light was propagated into the sensor from the opposite side as the interrogation light as shown in figure 16. The power laser, which was terminated in 110µm diameter multimode-fiber was simply fusion spliced to the double-clad fiber containing the sensor. At the junction of the double-clad and multi-mode fibers, the power light feeds into the inner cladding of the double-clad fiber. In turn, the metal coating on the sensor absorbs the evanescent power light and heats the coating. The fiber passes through the central chamber, which is covered by an outer steel chamber in order to provide insulation.

4.0 EXPERIMENTAL RESULTS

The Palladium coated FBG sensors were first tested as passive sensors (without applying optical power) at room temperature. Sensors were evaluated in varying ambient hydrogen conditions to allow characterization. Figure 17 shows the initial results obtained using a 150 nm Palladium-layer coated FBG and a 350 nm coated FBG. During this initial experiment, the chamber temperature was first stabilized at 22°C. Then, H_2/N_2 gas was flowed through the test chamber at a given concentration for 5 minutes before reading the center (or Bragg) reflected wavelength.

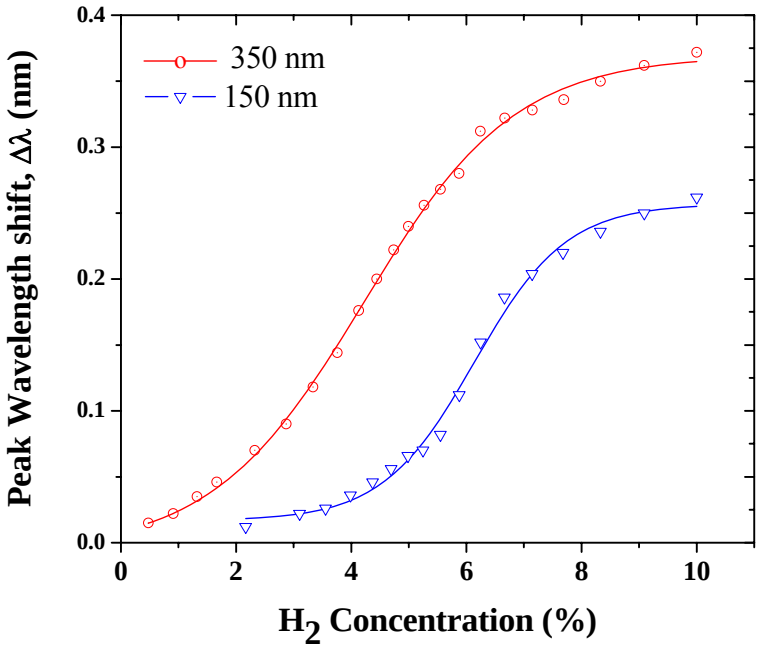

Figure 17: 150nm and 350nm Pd coated FBG responses in differing H_2 concentration indicating increased response using the thicker coating.

Several key pieces of information were gleaned from this initial test. Firstly, it was noted that the sensors exhibit a distinctly cubic response over H_2 concentration. Upon examination of the relevant literature, it was noted that as the partial pressure of the ambient hydrogen increases, the Palladium will undergo an to β phase change if the hydrogen/palladium atomic ratio goes beyond about .01 at room temperature. The phase transition in turn results in some degree of hysteresis, or uncertainty in the lattice constant, depending on whether the hydrogen content was increasing or decreasing to a particular level. It has been shown that a bi-directional hysteresis loop exists over the phase change region in which the H_2 concentration can not be definitively determined by the lattice constant of the Palladium [3].

Fortunately, this hysteresis region seems to occur beyond the lower explosion limit of the hydrogen, and well beyond the 1% lower detection limit sought for leak detection. Also, despite the lack of accurate H_2 concentration characterization over some small range (perhaps 4%-8%), a significant wavelength shift still occurs in this region, indicating no decrease in the ability of the sensor to detect leaks at these concentrations.

Figure 18 illustrates the reflection spectrum of 150nm and 350nm sensors at room temperature in the absence of H_2 and in the presence of 10% H_2. The latter was viewed as a "full scale" response of the sensor, beyond which characterization would not be necessary. Several key features should be noted herein. Firstly, the 350 nm sensor provides 0.37 nm of wavelength shift at full scale, while the 150 nm sensor provides about 0.2 6nm of wavelength shift. This shows a 42.3% better response for the 350 nm sensor at room temperature. This is an immediate indication that an optimal Pd thickness will be found at deposition thicknesses greater than 150nm. Although the initial indication is that thicker layers of Pd may perform better, no thorough stepwise characterization of thicknesses has been accomplished in this research, nor

has the durability of various thicknesses of coating been evaluated. In addition to the initial observations regarding the magnitude of wavelength shift, one will also note some change in the shape of the spectrum associated with the influx of H_2. This is undoubtedly due to some change in the overall shape of the grating as well as a general change in length. The absence of severe distortion in these spectra indicates that volume swelling of the Pd coating is occurring evenly. Repeatability of this experiment over a few tens of cycles indicates that the film exhibits good adhesion and structural integrity.

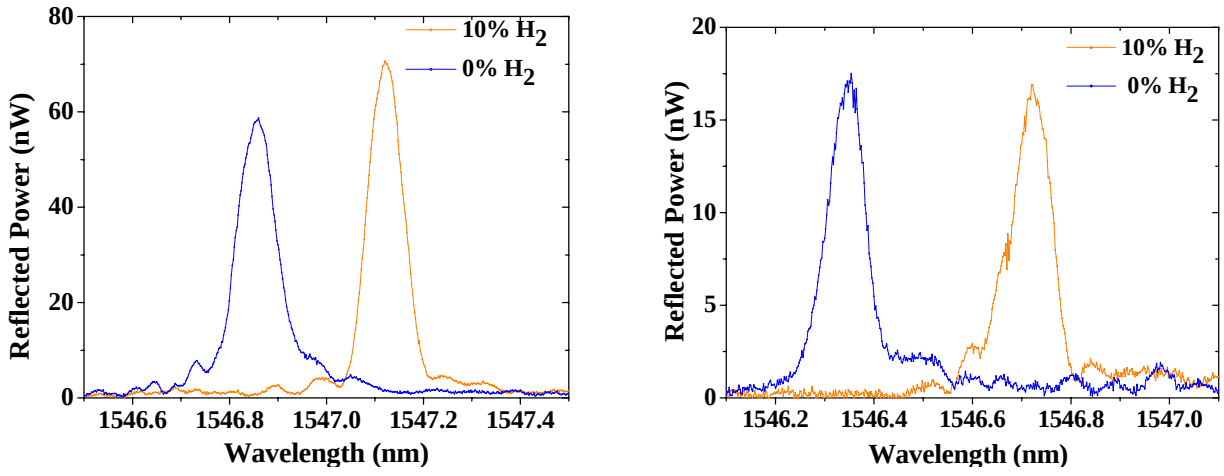

Figure 18: Reflection spectrum for two different thicknesses of Palladium coated FBGs at Room Temperature: (a) 150nm Pd coated FBG, and (b) 350nm Pd coated FB

More careful evaluation of the structural integrity of the Pd films was accomplished via SEM analysis of the film's grain structure. Figure 19 below shows two attempts at film construction during the design phase. The sensor on the right, on figure 19 (b), has poor adhesion of the Pd coating. The sensor on the left, on figure 19 (a), uses a Tantalum adhesion layer, and exhibits good adhesion properties. These results provide the basis for the continuation of use of Tantalum for adhesion. It should also be noted that the film exhibits a high degree of flatness

and continuity. The absence of cracking and other major deformities in the tantalum layered sample is a testament to the good quality of film production.

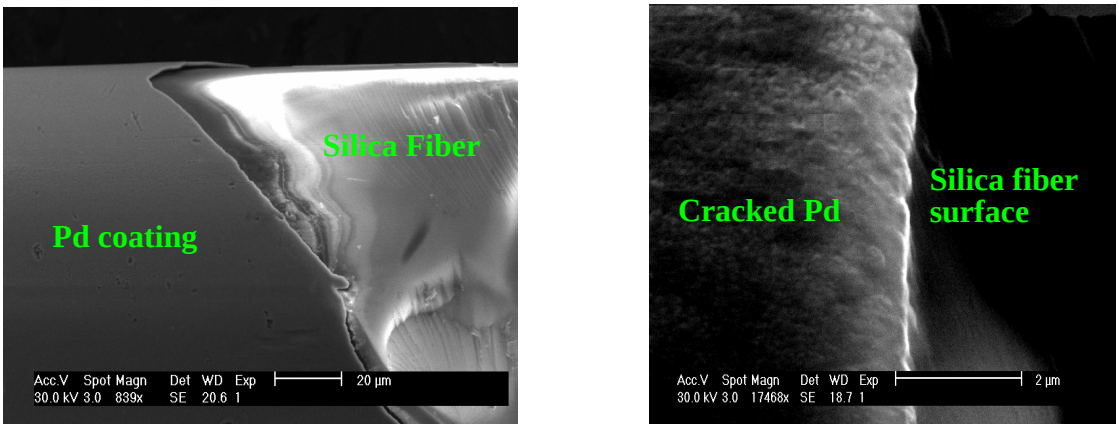

(a) (b)

Figure 19: Pictures of the Palladium coating on the FBG taken by Scanning Electron Microscope (a) a good coating, and (b) a broken surface on the coating

In order to fulfill the initial design criteria, it was necessary to verify the operation of the sensors at low temperatures for use near cold liquid H_2 storage tanks and pipes. Initially, problems arose with sensor operation at low temperatures, prompting the use of our unique laser-heating technique for improving sensor response.

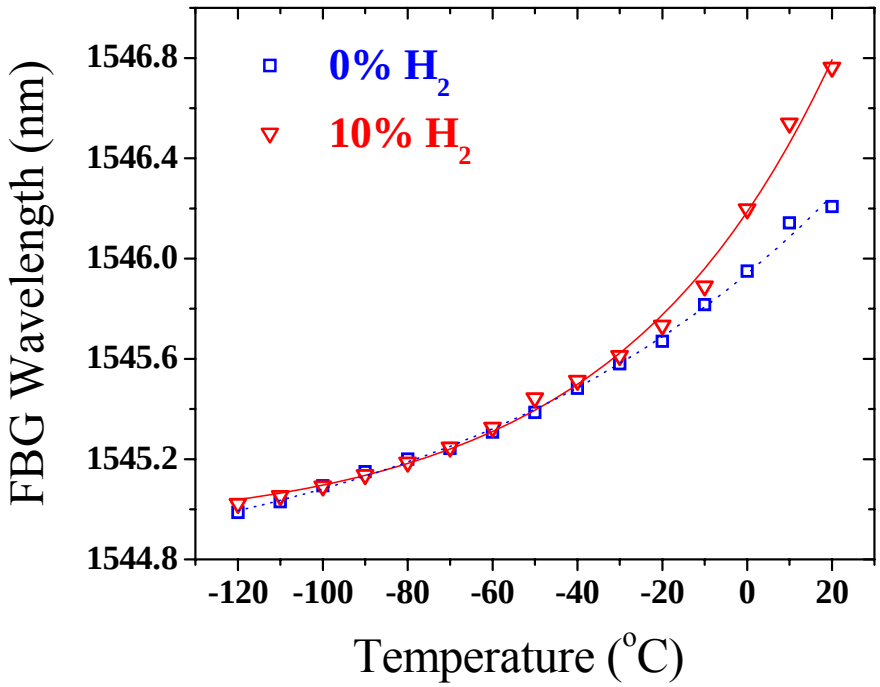

Figure 20: Two- minute H_2 exposure for a 150 nm Pd coated sensor over temperature.

Figure 20 clearly illustrates the problem associated with low temperature response. In the figure, a 150 nm sensor is exposed to 10% H_2 at low temperature. The center wavelength is recorded as the temperature is increased and stabilized for 2 minutes at each reading. Next, the same test was performed in the absence of hydrogen. Only at around -20°C does the presence of hydrogen reveal itself given the 2 minute exposure time. This is because the rate of hydrogen absorption decreases dramatically with a decrease in temperature. Although the full-scale response would be similar over the entire range of temperatures, the response time increases to a level far too high for any sort of leak detection application. The implementation of a technique that allows local remote heating of an on-fiber sensor provides an improvement of the sensor response.

Since we know that Pd-FBG sensors respond well at room temperature or higher temperatures, we can inject high-power laser light to heat the Pd-FBG sensor locally, facilitating rapid hydrogen diffusion and reaction with the Pd film in a cold environment. Once the saturation absorption is reached, the fiber is then rapidly cooled back to the environmental temperature to measure Pd-swell-induced FBG shift and determine the H_2 concentration.

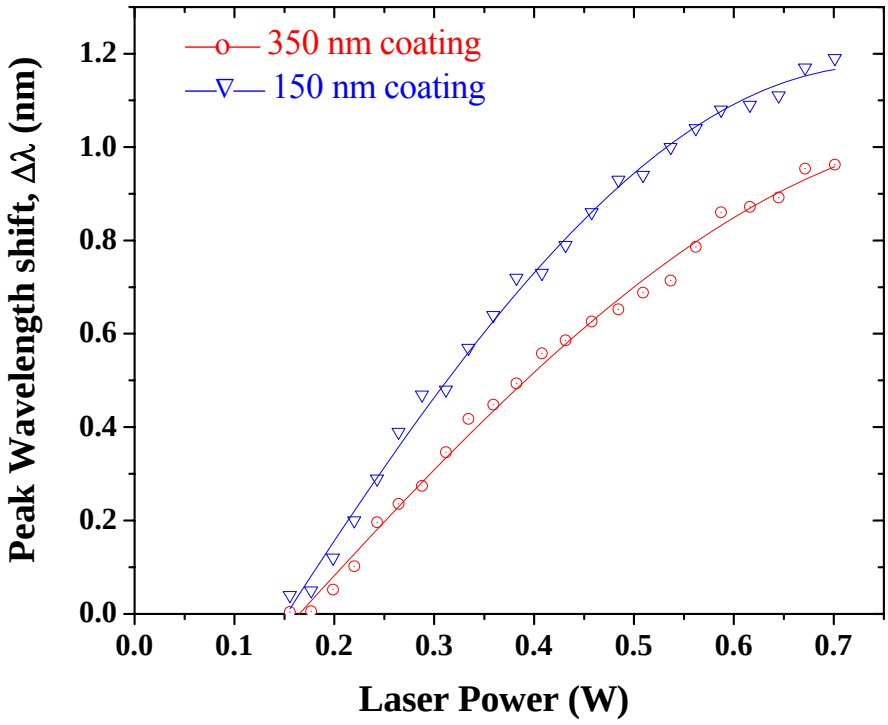

Figure 21: Laser heating response for 350nm and 150nm Palladium coated FBGs at Room Temperature.

In order to enable precise use of our laser sensor heating system, it was necessary to characterize the heating capabilities of the infrared heating laser. This was accomplished by increasing the laser power while measuring the sensor's reflected center wavelength in a room temperature environment. Figure 21 shows the resulting shift in center wavelength associated

with a given input laser power. It is worth pointing out that the laser heating efficiency is low due to a number of loss mechanisms. This is because a significant portion of laser power was lost at the junction of multimode fiber and double-clad fiber due to the mode mismatch (60%). In addition, the stripped length of the bare fiber containing the sensor is ~5 cm, although the length of the FBG is only 1 cm. To ensure the Pd-coating covers the entire FBG sensor, 4 cm of bare fiber was coated with metal. These extra lengths of coating and bare fiber dramatically reduce the heating efficiency. This problem could well be taken care by the use a much shorter FBG (3-4 mm). By reducing the Pd coating to 1 cm and recoating the bare fiber with low-index jacket material, one can expect to increase the heating efficiency by about one order of magnitude. With these simple improvements, 200-250^{o}C temperature increase above the ambient temperature could be achieved using about 100 mW of laser power.

Heating of the fiber sensors using in-fiber light provided the necessary means to improve the performance of the sensing system. By using in-fiber optical heating, a Pd-coating can be made to rapidly absorb and degas hydrogen at any temperature for rapid response. Figure 22 below shows the heated (full power) and unheated spectra produced by a 150nm sensor. Firstly, it was noted that some "chirp" occurred during heating which is a result of the laser power entering one side of the fiber, and decreasing in intensity as it travels along the coated section. For better accuracy, it is necessary to more accurately control the amount of power light absorbed by the Pd coating in order to both eliminate this chirping effect, and to allow precise control of the power absorbed by each sequential sensor in a long string of sensors on a single fiber.

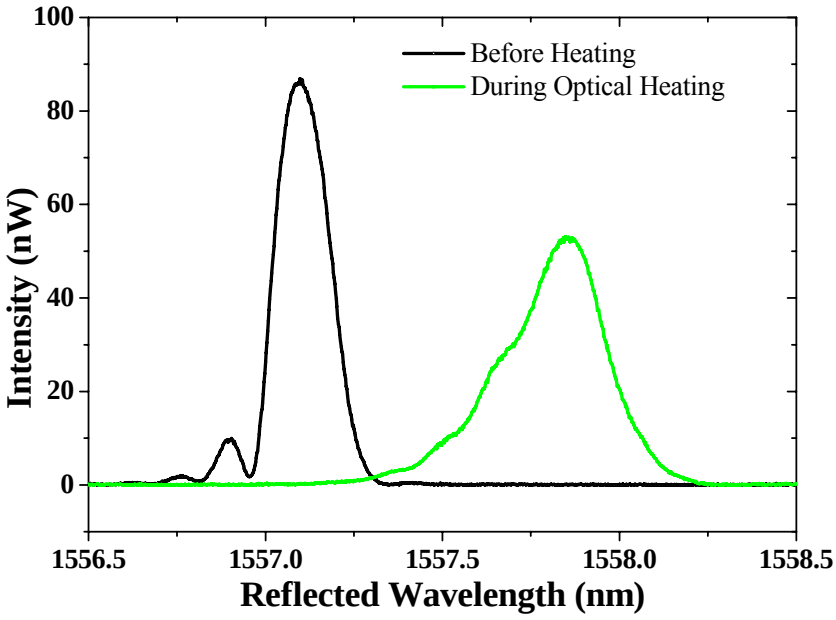

Figure 22: Heated and Unheated Spectra of 150nm Sensor

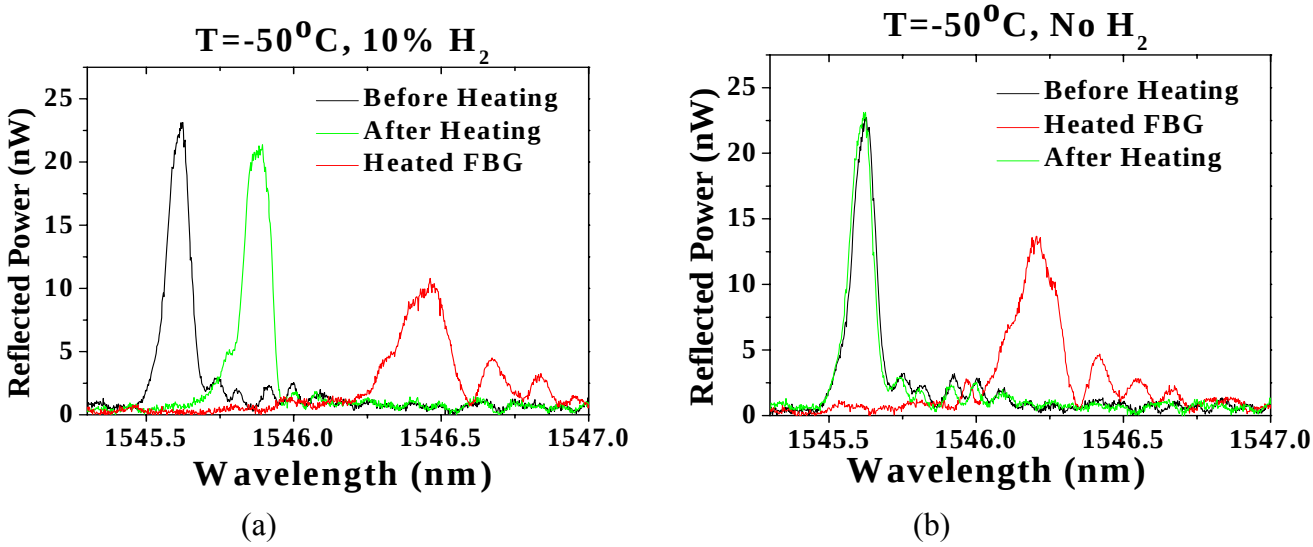

Figure 23: Sensor response at -50°C using laser heating: (a) with 10% H_2, and (b) without H_2.

After the ability of the laser heating system to locally regulate the temperature of a given sensor had been established, it was necessary to prove the utility of employing such heating for improving sensor response at low temperatures. Figure 23 above is a spectral illustration of the effectiveness of the technique. In the first test (a), the ambient temperature is brought to -50^{o}C, and a 10% hydrogen atmosphere is introduced. After several minutes, no wavelength shift is observed. This agrees with the results shown in figure 20. The Pd-FBG sensor shows no reasonable response to 10% hydrogen at this low temperature. The sensor is then heated with the infra-red laser, and the resultant spectral shift due to heating is shown in the red trace of figure 23 (a). The laser power is increased so that the temperature of the FBG is brought to room temperature (20^{o}C), where the sensor shows good response at 10% concentration. Once the saturation absorption is achieved, the laser is then turned off to allow the sensor to cool down to the environmental temperature of -50^{o}C. Given the small thermal mass, the cooling process is rapid and estimated to be less than 1 second. The hydrogen in the Pd-coating causes swelling at this temperature, stretching the FBG peak to the longer wavelength as shown in the green trace of figure 23 (a). Using this process, 10% hydrogen produces 0.21 nm FBG shift in a few seconds, which is a dramatic improvement from the passive hydrogen sensor that was demonstrated in figure 20.

As a control test (b), the hydrogen was then removed from the process and the laser heating was repeated. This resulted in the center wavelength shifting back to its -50^{o}C rest position, as seen in figure 23 (b). It is important to realize that the effect of the laser heating is simply to speed up the rate of absorption allowing quick measurement. No permanent effects were noted due to the heating, and given enough time at low temperatures, hydrogen will still in-gas or out-gas by itself.

It is worth noting that the 0.21 nm FBG shift using the optical heating process is 57% of the FBG shift at the room temperature. Since the Pd-coating absorbed hydrogen at the room temperature by local optical heating, we should expect a similar FBG shift given the same hydrogen concentration. However, this reduced FBG shift is probably due to the reduced elastic-optical coefficient of silica glass at low temperature. As further proof of the effectiveness of laser heating for low temperature sensor operation, the heating technique was used to characterize various concentrations of hydrogen at -50°C. These results are shown in figure 24 below.

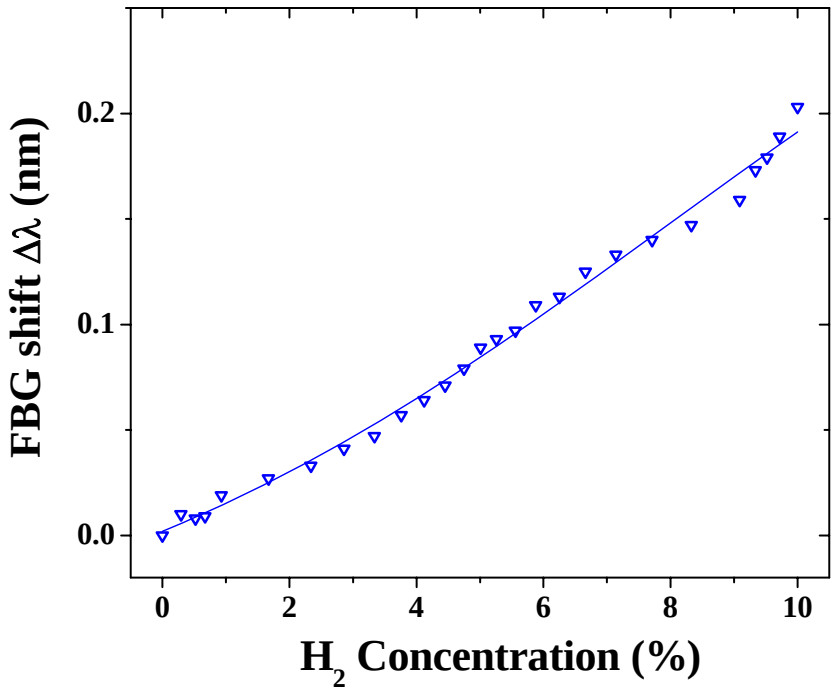

Figure 24: Sensor Response with Varying H_2 Concentration at -50°C with laser heating.

Initially, the ambient temperature was reduced to -50°C. Then, increasing quantities of hydrogen were introduced into the test chamber. At each concentration interval, laser heating was applied for 2 seconds, and the subsequent wavelength shift was recorded. As shown, the

shape of the concentration curve is somewhat similar to that at room temperature, and the full scale response is similar in magnitude. Differences in the film chemistry at this temperature may provide some indication as to the small physical differences therein. Most importantly, it was shown that hydrogen detection at low temperatures is possible using our laser heating system. Additionally, sensor response time may be improved at any temperature using the same system.

We also experimented on the multiplexing capability of the sensors. A schematic of the setup used for multiplexing is shown in figure 25.

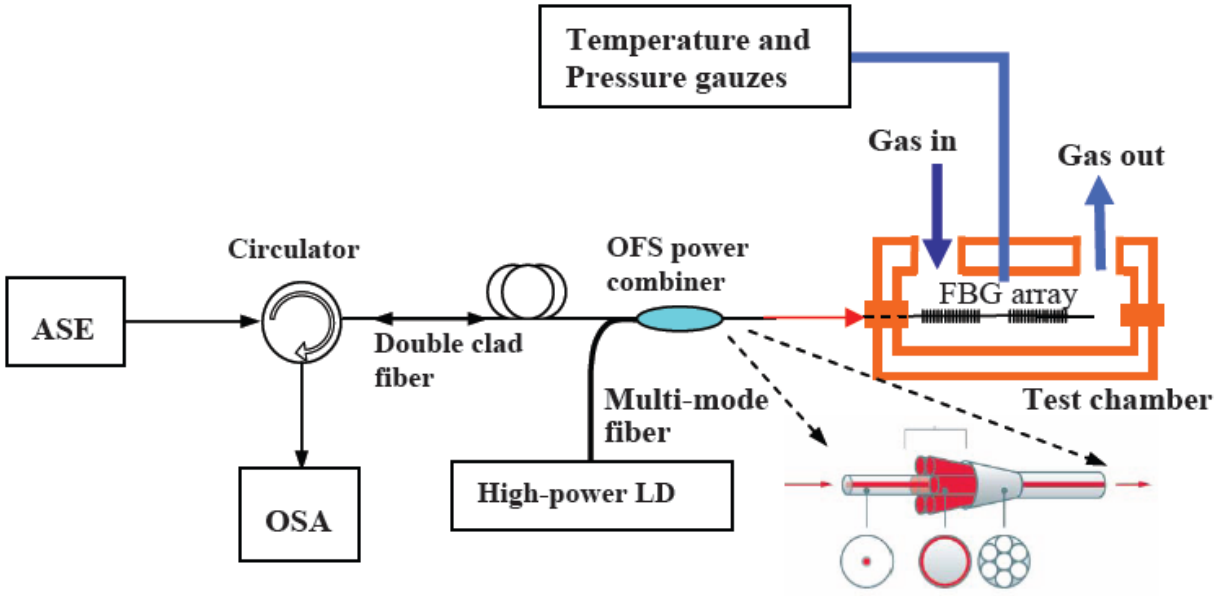

Figure 25: Proposed FBG sensor array in the double-clad (DC) fiber using a power combiner and a single fiber feed through. The sketch of the power combiner is from OFS website [26].

A double-clad fiber was used to deliver optical power to any point along the sensing fiber. The energy supply scheme demonstrated for hydrogen sensing in the previous works requires two fiber feed-throughs. Previously, sensing and power light were coupled from the

opposite ends of the fiber. However, using the setup shown in figure 25, a scheme was successfully implemented to launch the power light and sensing light from the same side of the fiber. A power combiner developed by the OFS laboratory (PowerMAX Combiner) was used, which was originally designed for high-power laser applications. The PowerMAX components can combine optical power from 6 to 18 multimode fibers and optical signals from 1 single-mode fiber into one double-clad optical fiber for use with a cladding pumped fiber. It provides an ideal solution for active fiber sensing applications. The one-side optical coupling, one fiber, and one feed through solution will significantly simplify the design, deployment, and maintenance of active fiber sensing networks. Using this scheme, we have successfully powered a Pd-FBG sensor. The result is shown in figure 26 below.

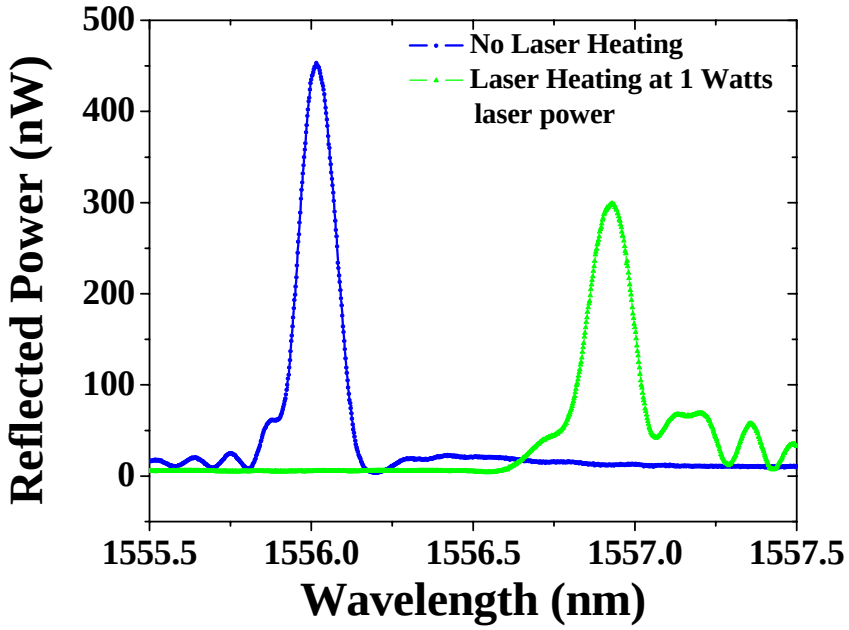

Figure 26: The heated spectrum of Pd-FBG sensor heated by a power laser using a power combiner.

Figure 27 below shows the FBG peak wavelength shift vs. the injected laser current using the setup with the power combiner.

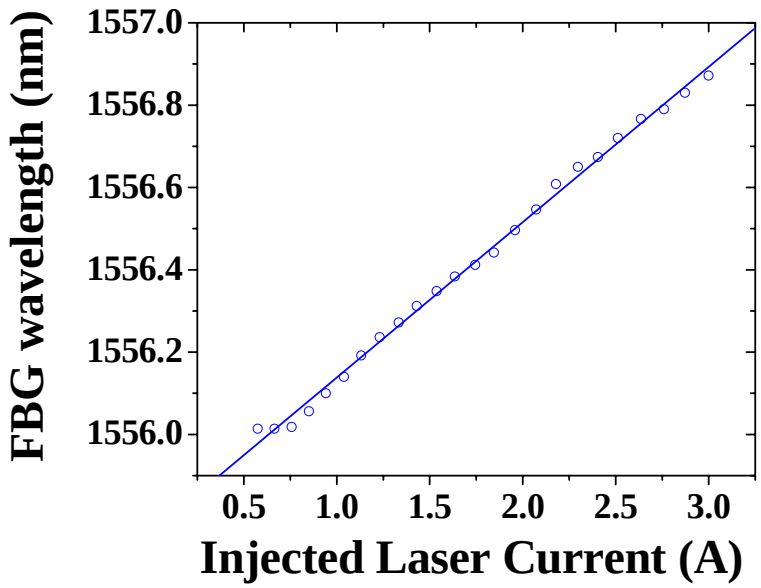

Figure 27: FBG peak shift as a function of injected laser current.

We were able to show that the optical heating technique is capable of heating a multi-sensor array simultaneously. This is demonstrated in figures 28 and 29.

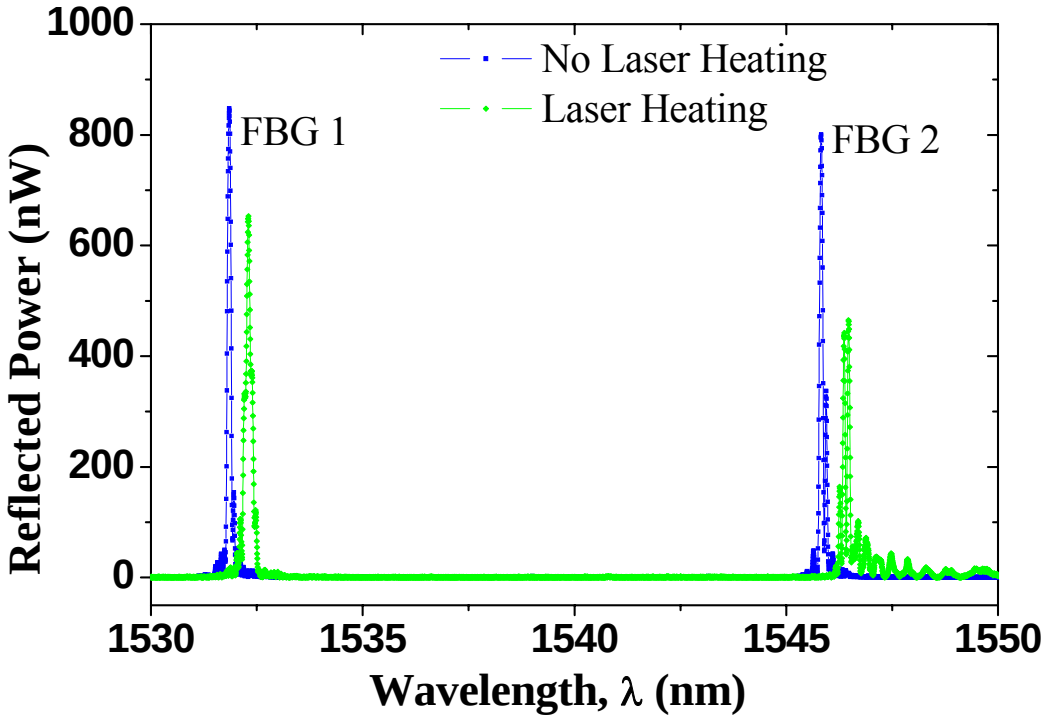

Figure 28: Two FBGs heated by in-fiber laser light. The power laser is launched from the FBG1 side.

The two multiplexed FBGs are inscribed in a double-clad fiber 1 meter apart. By adjusting the coating composition, we have achieved equal FBG wavelength shifts for both gratings.

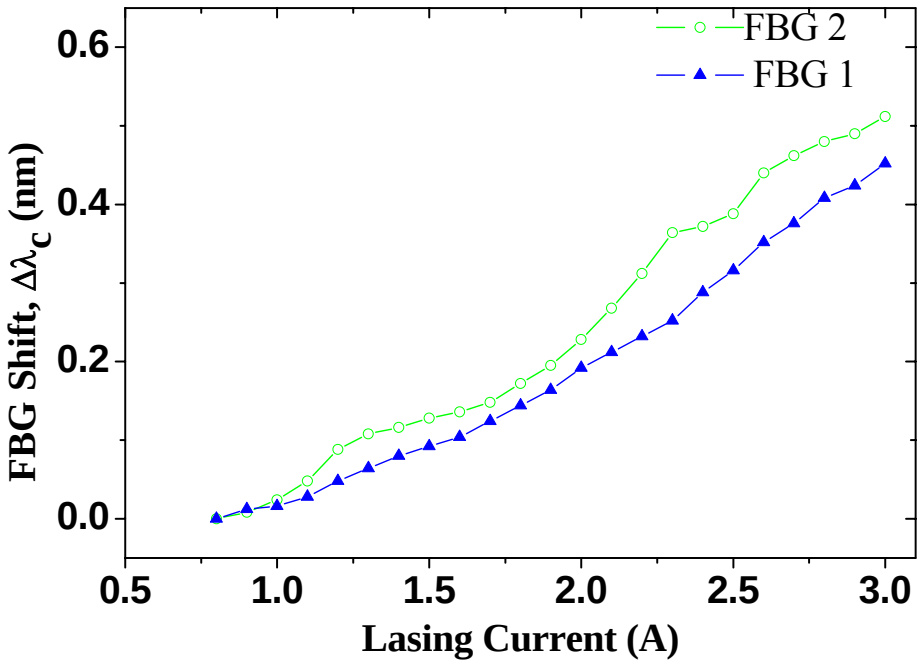

Figure 29: The FBG shifts as functions of input laser injection current

Figure 30 below shows multiplexing feasibility with 14 optical taps. The optical tap length of each tap is 1cm and the total fiber length is 2.5 meters. The fact that light passed through all the taps shows that numerous FBGs can be multiplexed for simultaneous sensing of hydrogen at various points along a chamber.

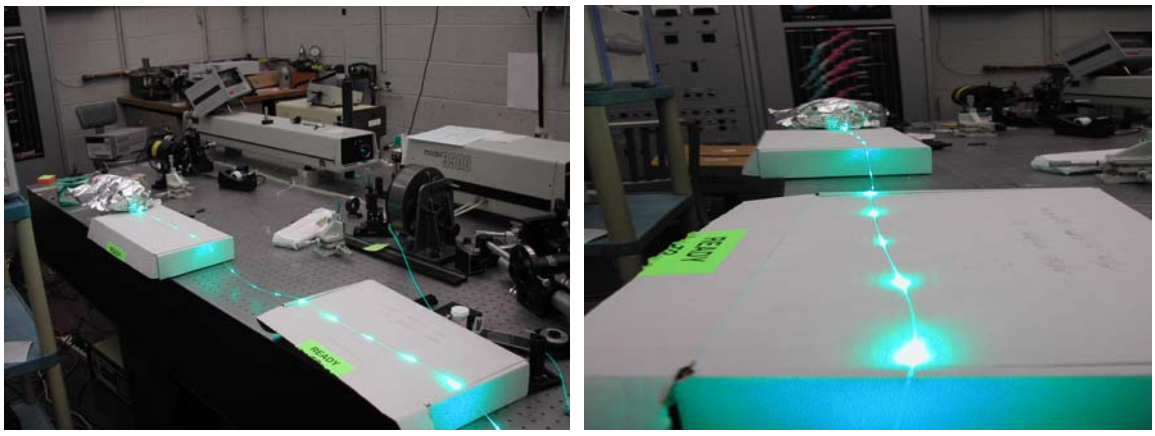

Figure 30: Multiplexing feasibility with 14 optical taps.

5.0 ANALYSIS AND CONCLUSIONS

We were able to show that for the 350nm Pd-coated grating, the response for 10% hydrogen was 0.37 nm shift in the peak of the reflected Bragg wavelength. The lowest tested hydrogen concentration was 0.5%, yielding 15 pm shift in the 350nm Pd-coated FBG. The measurement was repeatable and there was little hysteresis at room temperature and low hydrogen concentrations.

This work also demonstrates an effective means to enhance the low-temperature performance of Pd-FBG sensors using our in-fiber optical heating technique. By locally controlling the adsorption and degassing temperature of a Pd film, it is possible to shorten response time over a range of temperatures, thus, facilitating fast operation of the hydrogen sensor at all temperatures. The technique demonstrated in this thesis facilitates the construction of a FBG hydrogen sensor array with only one fiber and one feed-through. With the use of the laser light, the temperature of the on-fiber palladium film can be controlled and optimized for rapid hydride formation and rapid hydrogen sensing at all temperatures.

In this research, we have successfully demonstrated that an optically powered FBG is an excellent method to improve the Pd-FBG sensor performance at low temperatures, along with making it suitable for all-temperature operation.

This system has the potential to provide a sensor network with many point sensors using only one fiber feed through and minimum packaging. One interesting thing about this method of

hydrogen sensing is that the fibers can not only be used for optical signal delivery, but also as multi-functional cables to deliver optical power for on-fiber actuation. Multiplexing feasibility of the sensors was also successfully shown, with two FBG sensors one meter apart. We were able to heat both the FBGs with the high-power laser diode.

5.1 MAJOR ACCOMPLISHMENTS

To summarize, here are some of the major accomplishments of the research project:

- Passive H_2 detection at less than 0.5% hydrogen at room temperature in less than 30s using a 350nm coated sensor, without optical heating.
- Accurate hydrogen concentration characterization over an appropriate range of interest (-120^{o}C to +95^{o}C).
- Successful demonstration of in-fiber light powered active H_2 sensors with one fiber feed through.
- Use of optical heating to facilitate hydrogen absorption and degassing. Sensor response time was shortened to less than 2 seconds over the temperature range of interest.
- Dramatic improvements in sensor performance at low temperatures using optical heating.
- Laser heating demonstrated for a multi-sensor FBG array in one fiber.
- Successful demonstration of fiber optic scheme to power and interrogate an H_2 sensor array from one side of a fiber.

5.2 FUTURE WORK

Although the scope of this project was achieved, several important steps could be taken to add to the importance and efficiency of this work. Provided the necessary funding, the plan is to deliver a proven prototype optical hydrogen sensor for ground station fault and location detection in fuelling equipment. The sensor system should be able to produce a reliable alarm for the LEL (about 4% H_2) at a known location along the fiber path. The sensors would be individually identifiable by the wavelength location of their reflection peaks. We could work to make sure that the sensors work only on the basis of the strain caused by the swelling Pd or Pd alloy as it absorbs hydrogen, so the factors affecting other electronic sensors will not be a factor in this regard.

Since these FBG sensors for hydrogen sensing actually work because of the strain caused in the hydride through absorption of hydrogen, as well as through change in temperature, it is necessary that the sensing system be able to determine the actual shift in the wavelength caused only by the absorption of hydrogen as the H_2 concentration changes. To take care of this dual effect, hydrogen-independent temperature sensing FBG should be incorporated in the fiber next to each hydrogen sensor. The difference between the two sensors readings at each location would provide the accurate shift in the Bragg wavelength caused only due to change in hydrogen concentration. This would improve the sensitivity of the sensor system.

By reducing the length of each grating, we should be able to multiplex numerous FBGs into a single fiber. Also, the reduced length would provide better sensitivity to the sensors. We can, for example, try to achieve an increased sensitivity (using scanning laser) so that the system is able to detect around 0.01% H_2. We could also try to maintain a very low response time for the alarm signal. We have so far only tested with up to 10% H_2 concentration. Using proper

laboratory procedures and taking appropriate care, we could try to demonstrate a response for higher H_2 concentration as well, without destroying the sensor. We could also work to produce a sensor readily available in the market. In this case, we would have to be able to demonstrate a lifetime of around 1000 cycles of 4% H_2.

For multiplexing of the sensors, proper procedures will have to be taken to make sure that they work correctly. We can make sure that the heat taps will not weaken the fiber or compromise the quality of the FBGs. Each heat tap can remove up to a certain amount of power per length of the sensor. This would enable us to know how many sensors can be multiplexed along one fiber.

During this project, since our goal was just to produce a hydrogen sensing system that could be used in the laboratory without complete accuracy, we did not look into the best heating laser available in the market. For better sensitivity, and for a faster response time for the alarm, we could look into using different laser systems like the pulsed laser or the continuous wave laser system. We might even be able to enhance accuracy using a better power combiner and coupler.

If these sensors were to be made commercially available, we would have to develop reliable means to prevent overheating of individual sensors, and also develop procedures to detect and deal with fiber breaks and other potential malfunctions. We could integrate a software based hydrogen calibration system that would make the system more reliable and provide a good response time for a reliable alarm signal. Work could also be done in developing proper packaging and mounting system for the sensors so that it will be easy to install and remove as necessary. This would also make maintenance easier, if necessary at a later time. Since FBG

sensors are fragile, we could work on providing fiber-break protection and sensor over-temperature protection as well. This would enable us to lengthen the lifetime of the sensors.

We have not tested the sensors at very high pressure environments, and around certain chemicals. We could test them out and see how they perform. Various temperature and reference sensors as well as other kind of sensors like pressure and stress sensors could be multiplexed along the same fiber and tested for performance as well. Most importantly, we could develop hydrogen sensors that are inexpensive, reliable, durable, and easy to handle and install.

BIBLIOGRAPHY

[1]. A. Othonos and K. Kalli, F*iber Bragg Gratings, Fundamentals and Applications in Telecommunications and Sensing*, Artech House Publishing, Norwood, USA, (1999).

[2]. Alessandra Chiareli, *Troubleshooting fiber Bragg grating fabrication with modeling*, Fiber Optics & Electronics Technology Center, AOPC Sept. 10, 1999, www.ima.umn.edu/talks/workshops/9-9-10.99/chiareli/chiareli.pdf

[3]. F. A. Lewis, *The Palladium Hydrogen System,* Academic Press, NY (1967).

[4]. X. Bevenot, A. Trouillet, C. Veillas, H. Gagnaire, M. Clement, *Surface Plasmon resonance hydrogen sensor using an optical fiber*, Measurement Science and Technology **13**, pp.118-124, 2002.

[5]. K.O. Hill, et al., *Photosensitivity in optical fiber waveguides: Application to reflection filter fabrication*. Applied Physics Letters **32**(10): pp. 647-649, (1978).

[6]. A. D'Amico, A. Palma, and E. Verona, *Palladium-surface acoustic wave interaction for hydrogen detection*, Applied Physics Letters **41**, pp. 300-301, (1982).

[7]. I. Lundstrom, S. Shivaraman, C. Svensson, L. Lundkvist, *A hydrogen-sensitive MOS field-effect transistor*, Applied Physics Letters **26**, pp. 55-57, (1975).

[8]. M.C. Steele, B.A. MacIver, *Palladium/cadmium-sulfide Schottky diodes for hydrogen detection*, Applied Physics Letters **28**, pp. 687-688, (1976).

[9]. F. Favier, E. C. Walter, M. P. Zach, T. Benter, R. M. Penner, ***Hydrogen Sensors and*** *Switches from Electrodeposited Palladium Mesowire Arrays*, Science **293**, pp. 2227 (2001)

[10]. M. A. Butler, *Optical fiber hydrogen sensor*, Applied Physics Letters **45**, pp. 1007-1009, (1984).

[11]. X. Bevenot, A. Trouillet, C. Veillas, H. Gagnaire, M. Clement, *Hydrogen leak detection using an optical fibre sensor for aerospace applications*, Sensors and Actuators **B67**, pp. 57–67, (2000).

[12]. M. Tabib-Azar, B. Sutapun, R. Petrick, A. Kazemi, *Highly sensitive hydrogen sensors using palladium coated fiber optics with exposed cores and evanescent field interactions*, Sensors and Actuators **B56**, pp. 158–163, (1999).

[13]. J. Villatoro and D. M. Hernández, *Fast detection of hydrogen with nano fiber tapers coated with ultra thin palladium layers*, Optics Express **13**, pp. 5087-5092, (2005).

[14]. B. Sutapun, M. Tabib-Azar, A. Kazemi, *Pd-coated elastooptic fiber optic Bragg grating sensors for multiplexed hydrogen sensing*, Sensors and Actuators **B60,** pp. 27–34, (1999).

[15]. K.T.V. Grattan, B.T. Meggitt, *Optical Fiber Sensor Technology*, Kluwer Academic Publishers, Boston, (2000)

[16]. M Buric, *Wavelength modulation spectroscopic chemical sensing using a piezo-electric tunable fiber Bragg grating laser*, MS Thesis, University of Pittsburgh (2005).

[17]. K.P. Chen, P.R. Herman, and R. Tam, *Strong fiber Bragg grating fabrication by hybrid 157- and 248-nm laser exposure,* Photonics Technology Letters, IEEE **14**(2): pp. 170-172, (2002).

[18]. R. Kashyap, *Fiber Bragg Gratings*, Academic Press, San Diego CA, (1999).

[19]. G. Meltz, W.W. Morey, and W.H. Glenn, *Formation of Bragg gratings in optical fibres by transverse holographic methods*, Optics Letters **14**(15), pp. 823, (1989).

[20]. C.M. Davis, E.F. Carome, M.H. Weik, S. Ezekiel, E. Einzig, *Fiber optic Sensor Technology Handbook*, Optical Technologies, (1986).

[21]. K. Ito, T. Ohgami, *Hydrogen detection based on coloration of anodic tungsten oxide film*, Applied Physics Letters **60** ,pp. 938–940, (1992**).**

[22]. M.A. Butler, A.J. Ricco, *Chemisorption-induced reflectivity changes in optically thin silver films*, Applied Physics Letters **53**, pp. 1471–1473, (1988).

[23]. J. da Silva, H. Kalinowski, *Strain Studies in Electrical Energy Transmission Cables using an Optical Fiber Bragg Grating Sensor*, Microwave and Optoelectronics Conference, **1**, pp. 313-316, (6-10 Aug. 2001).

[24]. C.S. Goh, M. R. Mokhtar, S. A. Butler, Y. S. Sze, K. Kikuchi, and M. Ibsen, *Wavelength tuning of fiber Bragg gratings over 90 nm using a simple tuning package.* Photonics Technology Letters, IEEE, **15**(4), pp. 557-559 (2003).

[25]. A. Guemes, J.M. Pintado, M. Frovel, E. Olmo, A. Obst, 17th Intl. Conf. Optical Fibre Sensors, Proc SPIE **5855**, 1000 (2005).

[26]. *PowerMAX Combiners*, OFS Specialty Photonics Division website, http://www.specialtyphotonics.com/pdf/products/specialty/highpower/SM%20PowerMAX%20Combiners.pdf.

[27]. *Optical Fiber Sensors Guide*, Micron Optics Inc. website, (2005), http://www.micronoptics.com/pdfs/Micron%20Optics%20Optical%20Sensing%20Guide.pdf.

[28]. T. Inui, T. Komukai, and M. Nakazawa, *A wavelength-tunable dispersion equalizer using a nonlinearly chirped fiber Bragg grating pair mounted on multilayer piezoelectric transducers*, Photonics Technology Letters, IEEE,. **12**(12), pp. 1668-1670, (2000).

[29]. A. D. Kersey, M.A. Davis,H.J. Patrick, M. LeBlanc, K.P. Koo, C.G. Askins, M.A. Putnam, E.J. Friebele, *Fiber Grating Sensors*, Journal of Lightwave Technology, **15**(8), pp. 1442-1463, (1997)

[30]. A. Othonos, *Fiber Bragg Gratings*, Rev. Sci. Instrum., **68**(12), pp. 4309-4341, 1997.

[31]. W. Enfield, *Innovations in Micro-Analytical Systems for Oil and Gas Applications*, Sandia National Laboratories, ASME-Petroleum Emerging Technologies Forum, (2002).

[32]. G. W. Hunter, P.G. Neudeck, L.-Y. Chen, D.B. Makel, C.C. Liu and Q.H. Wu, D. Knight, *A Hazardous Gas Detection System for Aerospace and Commercial Applications*, 34th Joint Propulsion Conference and Exhibit (July 12–15, 1998).